Functional investigation of a transcriptional regulator *ptrA* from *Pseudomonas chlororaphis* PA23

by

Jason Hok Shun Chan

A Thesis submitted to the Faculty of Graduate Studies of

The University of Manitoba

in partial fulfilment of the requirements of the degree of

MASTER OF SCIENCE

Department of Microbiology

University of Manitoba

Winnipeg

ABSTRACT

Pseudomonas chlororaphis PA23 is a promising biological control candidate against *Sclerotinia sclerotiorum*, a fungal pathogen that causes stem rot in canola. A library of transposon mutants was previously created to understand the molecular mechanisms underlying the antifungal capabilities of PA23. A novel LysR-type transcriptional regulator, called PtrA, was identified as a key global regulator involved in secondary metabolite production. The function of PtrA at the molecular level was investigated in this thesis. Solubility problems encountered during the purification of PtrA redirected efforts to studying a truncated version of the protein instead. A two-step purification of the truncated protein, involving streptomycin sulfate precipitation and immobilized metal-ion affinity chromatography, yielded a highly pure protein. Preliminary crystal growth was achieved for the effector binding domain portion of PtrA. Transcriptional fusions suggested that essential regulatory binding sites of *ptrA* may lie somewhere between 52 and 198 bp upstream of the translational start site. The research presented in this thesis will help guide future functional studies on PtrA.

ACKNOWLEDGEMENTS

To my supervisors Teri and Peter, thank you for your encouraging support and guidance over the two years, and for allowing me the freedom and independence in conducting research and pursuing my personal goals. I aspire to take with me the same level of passion, work ethic, and professionalism that you exemplify every day. The same could be said of my committee members Dr. Brian Mark and Dr. Sean Mckenna. Your knowledge and generosity in caring about my research, as well as opening your lab to me as if I were one of your own students, is truly appreciated. My deep gratitude goes to Dr. Lynda Donald for your tremendous help and enthusiasm with the mass spectrometry experiments and analysis; Dr. Markus Meier for your technical expertise and assistance with analytical gel filtration; and Dr. Trushar Patel for your training and outstanding suggestions with dynamic light scattering and protein work. I would also like to thank the students and staff from the Microbiology department for not only being so kind and accommodating, but for making life in and outside the Buller building fun as well. Finally, to my lab mates Jack, Jacylyn, Vikash, Munmun, Tuhin, Carrie, Chrystal, Jer, and Natasha, thank you for your collective contribution and friendship—I will never forget my experience here.

TABLE OF CONTENTS

LIST OF FIGURES

LIST OF TABLES

LIST OF ABBREVIATIONS

A_{260} – absorbance at 260 nanometres
A_{280} – absorbance at 280 nanometres
A_{420} – absorbance at 420 nanometres
ABS – activation binding site
Amp – ampicillin
βME – β-mercaptoethanol
bp – base pairs
Cam – chloramphenicol
CHAPS – 3-[(3-cholamidopropyl)dimethylammonio]-1-px-ropanesulfonate
CV – column volume
DBD – DNA-binding domain
ddH_2O – double-distilled water
DLS – dynamic light scattering
DMSO – dimethyl sulfoxide
dNTPs – deoxynucleotide triphosphates
DNA – deoxyribonucleic acid
DNAse – deoxyribonuclease
DTT – dithiothreitol
E. coli – *Escherichia coli*
EBD – effector-binding domain
EDTA – ethylenediaminetetraacetic acid
EMSA – electrophoretic mobility shift assays
ESI – electrospray ionization
FPLC – Fast protein liquid chromatography
g - gravity
Gm – gentamicin
His – histidine
IMAC – immobilized metal-ion affinity chromatography
IPTG – isopropyl β-D-thiogalactopyranoside
Km – kanamycin
kDa – kilodalton
LB – Luria-Bertani
LH – linker helix
LTTR – LysR-type transcriptional regulator
mAu – milliabsorption units
MW – molecular weight
MCWO – molecular weight cut-off
MS – mass spectrometry

NDSB-195 – non-detergent sulfobetaine 195
Ni-NTA – nickel-nitrilotriacetic acid
Nm – neomycin
OD_{600} – optical density at 600 nanometres
ONPG – o-nitrophenyl-β-D-galactopyranoside
PAGE – polyacrylamide gel electrophoresis
PBS – phosphate buffered saline
PCR – polymerase chain reaction
PDB – protein data bank
PEG – polyethylene glycol
PEI – polyethyleneimine
PGPR – plant growth promoting rhizobacteria
PIA – Pseudomonas Isolation Agar
Pip – piperacillin
psi – pounds per square inch
ptrA – *Pseudomonas* transcriptional regulator A
QS – quorum sensing
RBS – regulatory binding site
RNAse – ribonuclease
rpm – rotations per minute
RT – room temperature
SDS-PAGE – sodium dodecyl-phosphate poly-acrylamide gel electrophoresis
SSR – sclerotinia stem rot
TAE – tris-acetate-EDTA
TB – Terrific broth
TBE – tris-borate-EDTA
TCEP – tris(2-carboxyethyl)phosphine
TE – tris-EDTA
TEMED – N, N, N', N'-tetramethyl-ethylenediamine
Tris – tris(hydroxymethyl)aminomethane
TSS – transformation and storage solution
UV – ultraviolet
V – volts
v/v – volume per unit volume
wHTH – winged helix-turn-helix
w/v – weight per unit volume

1. INTRODUCTION

1. 1. Biological control

Perhaps the most widely accepted and quoted definition of the term *biological control* is "the reduction in the amount of inoculums or disease-producing activity of a pathogen accomplished by or through one or more organisms other than man" (Cook and Baker, 1983). In agriculture, biological control was discovered by trial and error long before the term was first coined by Harry Smith in 1919. The earliest documented example is the ancient practice of crop rotation mentioned in Roman literature (White, 1970). In addition to restoring nutrients in the soil, alternating of crops over the years can help control soil-inhabiting plant pathogens and pests. Proponents of this approach report that biological control is a safe practice, more stable, and longer lasting than other methods of disease suppression (in Cook, Chairman; 1987; Waage and Greathead, 1988).

The other two cultural methods for controlling pests can be categorized as either physical or chemical. Physical control refers to changing the physical environment in order to eliminate pests or reduce their effects. Physical control methods include tillage, grazing, open-field burning, solar heating, or physical separation, including erecting barriers or choice of planting date. Chemical control involves the use of synthetic pesticides to eliminate pests. Physical and chemical control methods, however, are not without limitations or drawbacks. Public health and environmental concerns, potential for pathogens developing resistance, difficulty in creating disease-resistant crops, increasing energy costs, and the trend towards more intensive farming with less crop rotation have increased interest and research in biological control strategies.

1. 2. Canola

Canola is derived from rapeseed or brown mustard and is comprised of three species: *Brassica napus, Brassica rapa,* and *Brassica juncea*. Canola was first trademarked in the 1970s when Canadian plant breeders developed a new oilseed crop safe for consumption. For a crop to be called canola, it must have less than 2% erucic acid and 30 μmoles of glucosinolates (Canola Council of Canada, 1999). The oil from canola is contained within the seeds of a flowering plant. The seeds are crushed for its oil and the rest of the seed, containing high protein content, is processed into animal feed. Today, canola is the third largest source of vegetable oil in the world (USDA FAS, 2012). The canola industry alone contributes over 13 billion dollars annually to the Canadian economy. By 2015, canola is projected to become the largest crop produced in Canada in both weight and value (Canola Council of Canada, 2005).

1. 3. Plant defense mechanisms

Plants are sessile organisms that are constantly under attack by pathogens. Besides the passive protection provided by the cell wall and waxy cuticle, plants have innate defense mechanisms that can perceive and respond to pathogen attacks. Plant receptors can detect the presence of pathogens either through pathogen compounds (e.g. lipids, oligosaccharides, or signaling molecules) or their degradation products (Boller, 1995; Gómez-Gómez, 2004). The elicitor molecules are often constitutively expressed and essential for the pathogen, and are collectively called pathogen-associated molecular patterns (PAMPs). Upon recognition, plants respond by turning on pathogenesis-related genes. The signaling pathways involved are complex and still poorly understood, but key

players such as protein kinases (e.g. mitogen-activated protein kinases and calcium-dependent protein kinases), phospholipid-derived molecules (e.g. phosphatidic acid), and signaling molecules (e.g. nitric oxide, reactive oxygen species, salicylic acid, jasmonic acid, and ethylene) have been identified (McDowell and Dangl, 2000; Romeis, 2001; Laxalt and Munnik, 2002). Plant defensive responses include changes in ion fluxes, synthesis of reactive oxygen species, and hypersensitive cell death (Gómez-Gómez, 2004). Furthermore, delayed defensive responses include the production of antimicrobial compounds, cell wall fortification, and activation of systemic acquired resistance, which establishes broad spectrum resistance in other uninfected areas of the plant (Gómez-Gómez, 2004; Durrant and Dong, 2004). In general, successful infection of a plant occurs when the pathogen can counteract the plant's defensive response by evading detection or by infecting the plant rapidly before an adequate defense is mounted (Hammond-Kosack and Parker, 2003).

1. 4. *Sclerotinia sclerotiorum*

Sclerotinia sclerotiorum (Lib.) de Bary is a fungal pathogen that infects at least 408 plant species worldwide, including economically important crops such as cotton, tomato, sunflower, soybean, and rapeseed (Boland and Hall, 1994). Over 60 names have been used to describe the disease caused by *S. sclerotiorum* (Purdy, 1969). With respect to canola, the necrotrophic ascomycete causes sclerotinia stem rot (SSR) by killing host cells in order to absorb nutrients from dead tissue. Sclerotinia stem rot is one of the major contributors to the reduction of canola yield. In Manitoba, canola yield losses due to SSR range from 5-100% (Manitoba Agriculture, 2004); whereas the annual average

yield losses in the US and UK are reported to be 13.6% (Pope et al., 1989; Gao et al., 2009).

Sclerotinia stem rot is characterized by white or pale-grey lesions on the stem starting from the soil line to the upper branches and pods. In addition to the wide array of degradative enzymes including pectinases, cellulases, and proteases, *S. sclerotorium* also produces oxalic acid (Marciano et al., 1983; Riou et al., 1993). The secretion of oxalic acid acidifies the infection site, weakens the cell wall, and facilitates infection by modulating plant defenses such as oxidative burst and Ca^{2+}-dependent mechanisms of the plant (Marciano et al., 1983; Godoy et al., 1990; Cessna et al., 2000; Williams et al., 2011). Successful infection will cause the pods to ripen prematurely and eventually cause the canola plant to wilt and die as sclerotia invade the centre of the stem. Sclerotia are the primary long-term survival structures that overwinter and stay viable in soil for up to 8 years (Adams and Ayers, 1979). Airborne ascospores released from apothecia that germinate from sclerotia can travel several miles (Li et al., 1994), making management of *S. sclerotiorum* a difficult and recurring problem for farmers every year.

1. 5. Biological control against *S. sclerotiorum*

Over the past 40 years, virtually no improvements in *S. sclerotiorum* disease resistance have been achieved through traditional breeding practices. The majority of biological control research involving *S. sclerotiorum* has focused on parasitism by fungal antagonists (McLaren et al., 1996; Gerlagh et al., 1999; Shi et al., 2004). This work has led to the development of Contans®, a commercially available biological control agent containing the fungus *Coniothyrium minitans* (Hedke et al., 1999; Vrije et al., 2001). The

agent is applied to the soil and inhibits sclerotia carpogenic germination. For canola however, Contans does not improve yield and the results are less consistent compared fungicides (McQuilken et al., 1995).

1. 5. 1. Plant growth promoting rhizobacteria

Plant growth promoting rhizobacteria (PGPR) are naturally occurring soil bacteria that colonize plant roots (Weller, 1988). The bacteria enhance plant growth and confer protection to their plant hosts through three main modes of action: competitive exclusion, antagonism, and the induction of plant immune responses (Haas and Défago, 2005). A major advantage of PGPR is that the plant immune system, once induced, will remain active for prolonged periods even if the inducing PGPR population declines (van Loon et al., 1998). Taken together, these traits of PGPR make them promising candidates for biological control agents. To date, PGPR species from the genera *Bacillus, Streptomyces, Burkholderia, and Pseudomonas* have been marketed as biological control agents (Saharan and Nehra, 2011).

Research focused on bacterial-mediated biological control of *S. sclerotiorum* has been less extensive and predominately performed on crops other than canola. *Pseudomonas* and *Bacillus* spp. have been extensively studied and are capable of antagonizing *S. sclerotiorum* and inducing systemic resistance (Walsh et al., 2001; Jiang et al., 2007; Ren et al., 2007; Li et al., 2011). Mechanisms of control include competing for nutrients, producing chitinase, lytic enzymes, siderophores, and antibiotics (Ganeshan and Kumar, 2005; Zhang et al., 2007; Fgaier and Eberl, 2011), and strengthening of the cell wall (Chen et al., 2000). In 2004, Savchuk and Fernando reported that two bacterial

isolates, *Pseudomonas chlororaphis* PA23 and *Pseudomonas* sp. DF41 were able to control SSR in field studies. More recently, *Pseudomonas fluorescens* P13 has also been shown to control SSR infection on canola in the field (Li et al., 2011).

1. 5. 2. Current management of *S. sclerotiorum*

To date, no cultivar of canola that is fully resistant to *S. sclerotiorum* infection exists. Canola cultivars demonstrating partial resistance have been reported in the literature (Zhao et al., 2004), but the biochemical and genetic basis for *S. sclerotiorum* resistance are not well understood. Enhancing resistance to fungal diseases in plants continues to be a major challenge for plant breeders and biotechnologists. This is particularly so when there is a lack of genetic sources of pathogen resistance and when resistance is governed by multiple genes (Fuller et al., 1994; Zhao and Meng, 2003; Liu et al., 2005; Zhao et al., 2007).

Crop rotation, using healthy seeds, and avoiding water logging, have so far proved unreliable or impractical in controlling SSR (Williams and Stelfox, 1980; Morrall and Dueck, 1982, Nelson, 1998; Abd-Elgawad et al., 2010). The primary approach for farmers to combat SSR is through the use of fungicides. Farmers are challenged with the decision of determining whether or not it is economical to use fungicide, which must be sprayed pre-emptively before visible SSR symptoms appear. Even then, results can be highly variable (Bradley et al., 2006) and efficacy decreases over time (Yu et al., 2002). Known adverse effects on non-target organisms have also been demonstrated (McGrath, 2001), resulting in one fungicide being removed from the market (Gilmour, 2001). The

failure of current pest control methods and concerns over pesticide use have prompted interest in finding alternative strategies for managing *S. sclerotiorum*.

1. 5. 3. *Pseudomonas chlororaphis* PA23

Pseudomonas chlororaphis strain PA23 is a biological control agent initially isolated from soybean root tips (Savchuk and Fernando, 2004). When delivered as a double foliar application, PA23 shows significant disease suppression of *S. sclerotiorum* by inhibiting ascospore germination on petals during a two-year field study (Fernando et al., 2007). Significantly higher levels of plant defence-related enzymes and compounds are present in canola when treated with PA23 (Nakkeeran et al., 2006). The enhanced accumulation of pathogenesis-related proteins and oxidative enzymes, including chitinase and β-1,3-glucanase, may contribute to the reduction in disease infection (Fernando et al., 2007).

PA23 produces a number of secondary metabolites that are believed to contribute to its biological control properties. These metabolites include phenazines, pyrrolnitrin, proteases, lipases, hydrogen cyanide, siderophores, and acetamido anthranilic phenol (Poritsanos et al., 2006; Zhang et al., 2006; Fernando et al., 2007; Selin et al., 2010). Further work by Selin et al. (2010) shows that pyrrolnitrin is the primary antibiotic responsible for controlling *S. sclerotiorum.* Elucidating the pathways of secondary metabolite production and how PA23 might affect innate plant defense mechanisms are ongoing areas of research.

1. 6. Regulation of secondary metabolites

Regulation of secondary metabolites in *Pseudomonas* spp. is under control of the GacS/GacA signal transduction system (Heeb and Haas, 2001), quorum-sensing (QS) circuits (Whiteley et al., 1999; Chin-A-Woeng at al., 2001), and the stationary phase sigma factor RpoS (Suh et al., 1999; Ge et al., 2007). There is also the potential for these systems to cross-regulate each other, but the level of cross-talk between the systems appears to be organism-dependent. For example, in *P. aeruginosa*, RpoS exerts both a positive and a negative effect on the QS genes *lasR* and *rhlR*, respectively (Schuster et al., 2004). In *P. chlororaphis* PCL1391, RpoS positively regulates the production of QS signaling molecules (Girard et al., 2006), whereas in *P. putida*, RpoS negatively regulates the QS genes *ppuI* and *rsaL* (Bertani and Venturi, 2004).

1. 6. 1. GacS/GacA

The Gac two-component system activates transcription of non-coding small RNAs collectively called Rsm, acronym for regulator of secondary metabolism (Liu et al., 1998). The Gac/Rsm system appears to be at the top of the regulatory hierarchy of secondary metabolite production (Chancey et al., 1999; Chin-A-Woeng et al., 2000; Duffy and Défago, 2000; Haas and Keel, 2003). The translational repression of target genes, mediated by mRNA-binding proteins associated with the Gac/Rsm system, is alleviated upon binding of non-coding small RNAs to the Rsm proteins (Lapouge et al., 2008).

The Gac system is known to play a role in the biosynthesis of QS signalling molecules (Reimmann et al., 1997). In *P. fluorescens*, where no QS signaling molecules

are known to be produced, the Gac system still positively regulates secondary metabolite production (Heeb et al., 2002). As with other pseudomonads, a mutation in *gacS* or *gacA* in PA23 results in the loss of antifungal activity (Poritsanos et al., 2006).

1. 6. 2. RpoS

The expression of stationary phase genes is dependent on the sigma factor RpoS. RpoS plays a role in the production of secondary metabolites, but the genes that it regulates varies depending on the organism. For example, in *P. fluorescens* CHA0, RpoS downregulates the expression of pyluteorin and 2,4-diacetylphloroglucinol (Schnider et al., 1995) but upregulates the expression of pyrrolnitrin, proteases, and HCN (Sarniguet et al., 1995; Haas and Keel, 2003); whereas in *P. chlororaphis* PCL1391, RpoS upregulates the expression of phenazines (Girard et al., 2006). In PA23, RpoS downregulates the expression of pyrrolnitrin, lipases, and proteases and upregulates the expression of phenazines (Manuel et al., 2012).

1. 6. 3. Quorum sensing

For many pseudomonads, production of exoproducts is under QS control. This cell-to-cell communication mechanism, mediated by diffusible signaling molecules, allows cells to alter their gene expression profiles in response to population density. In terms of secondary metabolite production by biological control strains, the Phz QS system controls the expression of phenazine production in *P. chlororaphis* and *P. fluorescens* (Wood and Pierson, 1996; Chin-A-Woeng et al., 2001; Khan et al., 2005). Moreover, a second QS system, called Csa, affects the production of protease in *P.*

chlororaphis 30-84 (Zhang and Pierson, 2000). In PA23, the production of phenazines and pyrrolnitrin is under the control of QS, and evidence of cross-regulation between QS and RpoS exists (Selin et al., 2012).

1. 6. 4. Abiotic factors

The availability of nutrients and other abiotic factors (e.g. pH, temperature, and oxygen) affect the production of secondary metabolites (Duffy and Défago, 1999; van Rij et al., 2004). Carbon and nitrogen sources and aromatic amino acids stimulate the production of phenazines, pyoluteorin, and 2,4-diacetylphloroglucinol (Duffy and Défago, 1999). Minerals and inorganic phosphates also affect the biosynthesis of secondary metabolites, in both an inhibitory and non-inhibitory manner depending on the *Pseudomonas* spp. (Slininger and Shea-Wilbur, 1995; Duffy and Défago, 1999).

1. 6. 5. LysR-type transcriptional regulators

Members of the LysR-type transcriptional regulator (LTTR) family play key roles in the regulation of secondary metabolites. For example, in *P. aeruginosa* PA14, MvfR activates transcription of the phenazine operon, autoinducer signaling molecules, elastase, and phospholipase (Cao et al., 2001). In *P. chlororaphis* PA147-2, FinR regulates antifungal metabolite production (Silby et al., 2005). In *Pseudomonas* sp. M18, PqsR and PltR regulate pyoluteorin and phenazine production (Yan et al., 2007; Huang et al., 2008).

1. 6. 6. *ptrA*

During the screening of a PA23 transposon library, a mutant lacking antifungal activity was identified (Poritsanos, 2005). The interrupted gene encoding a LTTR is designated *ptrA* (*P*seudomonas transcriptional regulator A). The *ptrA* mutant exhibits a dramatic phenotype, which includes the loss of phenazine, pyrrolnitrin, and quorum sensing autoinducer production, reduction in hydrogen cyanide, protease, and lipase activity, and altered motility and biofilm formation (Poritsanos, 2005; Selin and de Kievit, unpublished). PtrA appears to be a key global transcriptional regulator in PA23 that is high up in the hierarchy of secondary metabolite regulation. The regulatory role of PtrA including the genes under its control has yet to be determined.

1. 7. The LTTR family

The LTTR family is the largest known family of prokaryotic transcriptional regulators. LysR, a transcriptional activator of *lysA*, was the best characterized protein of the family at the time of study and subsequently became the family namesake (Henikoff et al., 1988). The LTTR family, identified based on similar amino acid sequences, is comprised of more than 80,000 potential members (IPR000847 HTH_LysR) as of this writing (Hunter et al., 2012). They are ubiquitously found in both gram-negative and gram-positive bacteria, as well as archaea (Sun and Klein, 2004; Maddocks and Oyston, 2008). In extreme examples, some bacterial genomes encode for more than 100 putative LTTR proteins, such as in *P. aeruginosa* PAO1. In contrast, LTTRs are absent from the genome of *H. pylori* (Knapp and Hu, 2010).

LTTRs are global transcriptional regulators that act as repressors or activators for single or operonic genes. They regulate an extremely diverse set of genes, such as those involved in basic metabolism (van den Bergh et al., 1993), stress-response (Li and He, 2012), quorum sensing (O'Grady et al., 2011), antibiotic resistance (Lindquist et al., 1989), and virulence (Kovacikova and Skorupski, 1999). LTTRs are often divergently transcribed from their target genes but they can be found elsewhere in the chromosome. They interact with co-inducer molecules that presumably affect DNA binding through conformational changes, which is generally required for transcriptional activation of target genes. For example, a conformational change is believed to be induced in OccR upon binding of octopine, a metabolite of the regulated octopine catabolism pathway, resulting in DNA bending relaxation and release of the –35 box (Akakura and Winans, 2002a, b). As such, co-inducers often form a feedback loop to control the autoregulation of the LTTR and its transcriptional regulatory activity (Picossi et al., 2007).

LTTRs are approximately 300 amino acids in length consisting of two domains: a N-terminal DNA-binding domain (DBD) and a C-terminal effector binding domain (EBD), which is also described in the literature as the regulatory domain, the inducer binding domain, the oligomerization domain, or the co-factor domain. The DBD consists of a winged helix-turn-helix (wHTH) DNA binding motif of approximately 60 amino acids. The conserved sequence of the N-terminal DBD helps identify LTTR family members. A flexible linker helix (LH) of approximately 20-30 amino acids joins the DBD to the EBD. The EBD shows greater sequence diversity but shares a common domain organization and structure. The binding site of the co-inducer generally lies between two Rossman fold-like subdomains within the EBD connected by a flexible

hinge region consisting of two anti-parallel β-sheets (Maddocks and Oyston, 2008). Despite common structural folds, LTTRs exhibit differences in oligomerization and promoter recognition.

1. 7. 1. Oligomerization states of LTTRs

The active form of LTTRs is generally believed to be a tetramer (Tropel and van der Meer, 2004; Maddocks and Oyston, 2008). The majority of full-length LTTRs that have been successfully crystallized confirm previously reported findings that they form tetramers. The tetramers are composed of two EBD dimers further oligomerizing to form a tetrameric EBD core, flanked by dimeric wHTH DNA-binding units. The two protomers forming a dimer are often arranged in a head-to-tail fashion (Maddocks and Oyston, 2008).

Based on the available structural data, Momany and Meldle (2012) propose three schemes of LTTR oligomeric organization. Scheme 1 regulators form a tightly packed tetramer using contacts between EBDs from two dimers. Scheme 2 regulators are held together by contacts made by both the EBD and LH, forming a more open conformation. Scheme 3 regulators are formed by interactions between heterodimers.

Variations within the core region of LTTR tetramers, composed of EBDs, also exist as revealed by crystal structures. In CbnR (Muraoka et al., 2003) and co-inducer-free DntR (Smirnova et al., 2004), the core is tightly packed with alpha helices from the second subdomain of the two EBDs coming into contact as part of the tetramer interface. In TsaR (Monferrer et al., 2010) and ArgP (Zhou et al., 2010), the same alpha helices do not interact with each other and the tetramer subsequently adopts a more expanded

conformation. In a putative LTTR protein from *P. aeruginosa* PAO1, the two dimers forming a tetramer lay on top of each other, resulting in a greater surface area being buried compared to the latter two structures (PDB code 3FZV, unpublished).

Interestingly, higher order oligomerization may be possible. Octamer assembly is shown in the crystal structure of CrgA (Sainsbury et al., 2009). Higher order beyond that of a tetramer is postulated for ThnR (Lopez-Sanchez et al., 2009) and BenM (Ezezika et al., 2007b). Taken together, the findings suggest that multimeric states other than dimers and tetramers may exist. The formation of heteromers may also be possible. In a paper published by Knapp and Hu (2010), the authors show that some LTTRs from *E. coli* K-12 could interact with non-cognate LTTRs.

The crystal structures of many truncated versions of LTTRs lacking the DBD have been solved. For a few of these LTTRs that have been truncated, the full-length structures have also been solved. For example, based on the crystal structures of the full-length and truncated versions of BenM (Ruangprasert et al., 2010), it is suggested that the BenM tetramer adopts different conformations upon co-inducer binding, but this has yet to be proven as the full-length LTTR structure is not bound to a natural co-inducer. The functional role of the different LTTR oligomerization states remains unclear.

1. 7. 2. LTTR transcriptional regulation

LTTRs commonly bind to a repressor binding site (RBS) located between positions –65 and +20 bp, overlapping the promoter of the divergently regulated gene. The RBS is sufficient for negative autoregulation and contains a LTTR box characterized by imperfect palindromic symmetry with a loose T-N_{11}-A consensus sequence. The

LTTR box varies in base pair composition and length (13-17 bp), and is present only in the RBS (Parsek et al., 1994). A second lower-affinity site, the activator binding site (ABS), is near or overlaps the -35 promoter box with no conserved sequence but is required for transcriptional regulation of the target promoter (Schell, 1993; Maddocks and Oyston, 2008). The LTTR binds to the RBS in the absence of a co-inducer. Upon binding with a co-inducer molecule, the LTTR will bind to a secondary site, the ABS, and activate transcription. As shown in Figure 1-1, this type of transcriptional regulatory mechanism constitutes the Group 1 regulators proposed by Picossi et al. (2007).

DNase I protection assays show that LTTRs often protect 50-60 bps of DNA (Muraoka et al., 2003; Akakura and Winans, 2002a, 2002b). Studies have indicated that LTTRs can cause DNA bending of up to 100° in order to repress transcriptional activation of the promoter. The degree of bending is determined by the presence or absence of the co-inducer molecule. Subsequent relaxation of DNA bending will activate transcription of target genes. A second group of LTTRs function by binding to multiple sites within the intergenic region (Fisher and Long, 1993; Hryniewicz and Kredich, 1995; Parsek et al., 1995; Pineiro et al., 1997). For example, AtzR binds to both a RBS and ABS′ in the absence of a co-inducer and causes DNA bending (Porrúa et al., 2007). Binding of the co-inducer will shift LTTR binding from one ABS′ to a second ABS″ further upstream, ultimately relaxing DNA bending and allowing for the recruitment of RNA polymerase. As shown in Figure 1-1, these Group 2 regulators follow the "sliding dimer model" proposed for the LTTR family (Toledano et al., 1994; Wang and Winans, 1995).

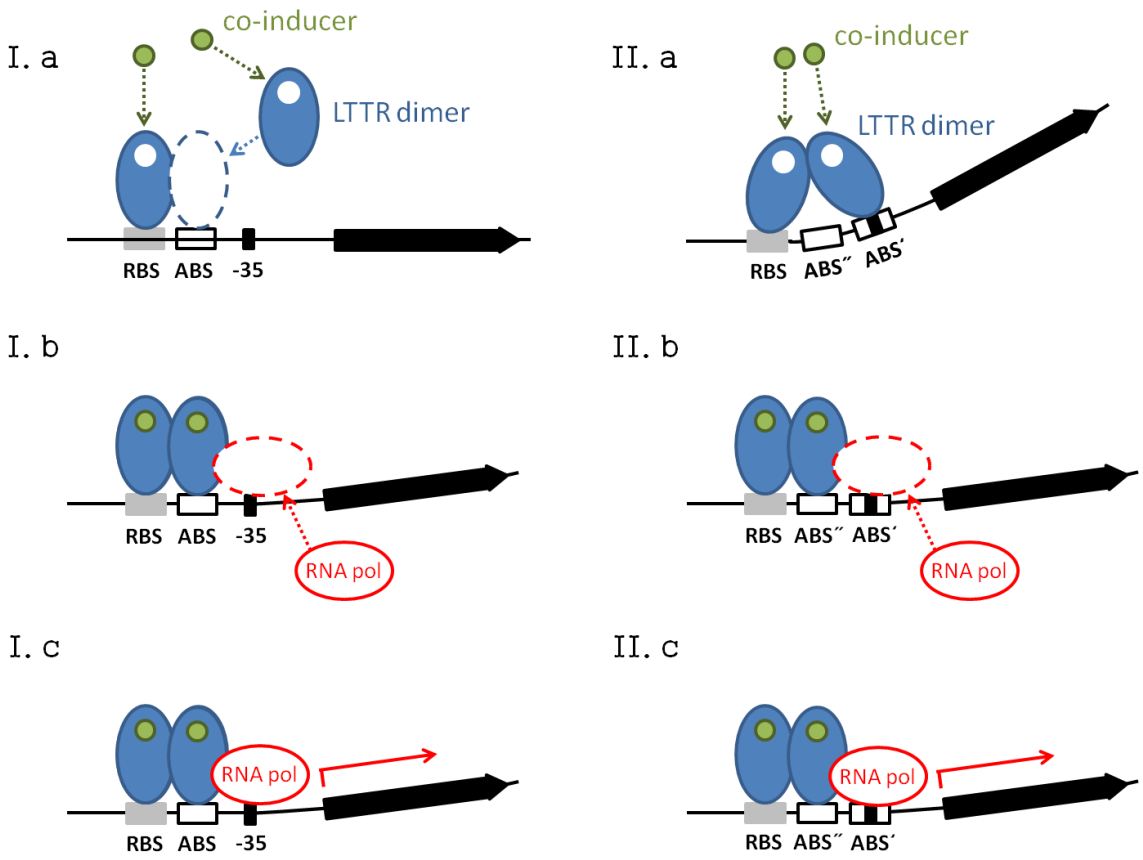

Figure 1-1. **A schematic representation of Group I and II type LTTRs binding at the RBS and ABS sites in LTTR-dependent transcriptional activation.** (**I. a**) In Group I LTTRs, the apo-form of a LTTR-dimer is bound at the RBS. (**I. b**) Upon binding with co-inducers, a second LTTR dimer binds to the ABS and forms a tetramer, (**I. c**) allowing for the recruitment of RNA polymerase and transcriptional activation. (**II. a**) In Group II LTTRs, apo-form LTTR-dimers form a tetramer and prevent transcription by blocking the -35 promoter box with binding at the RBS and ABS′. (**II. b**) Upon binding with co-inducers, DNA bending of the promoter region is relaxed as the first ABS′ binding site is released and the holo-form LTTR tetramer binds to the second ABS″. (**II. c**) RNA polymerase is recruited and transcription of the target gene is activated.

1. 7. 3. LTTR autoregulation

The mechanism of LTTR autoregulation is even less understood than LTTR regulation of target genes. It is believed that the LTTR box is necessary for autoregulation. A small number of LTTRs bind as dimers in the absence of co-inducers, centered approximately at position −62, and as tetramers in the presence of co-inducers bound at positions −62 and −42 (Schell and Poser, 1989; Parsek, 1992; Lorenz and Stauffer, 1995). It is suggested that LTTRs autoregulate their own transcription as a dimer by binding to the LTTR box, whereas the tetrameric form is required for divergent regulation of target genes. The multimeric state of LTTRs is believed to be influenced by the presence or absence of co-inducers. However, there is no clear evidence to date supports this claim. The mechanism of LTTR autoregulation is even more ill-defined for target genes that are not divergently transcribed. For these non-divergently regulated genes, the intergenic regions have not been characterized at the genetic level. It is not known whether a LTTR box exists and DNA-binding assays have not been performed (Maddocks and Oyston, 2008).

1. 7. 4. LTTR crystal structures

Solubility issues associated with purifying LTTRs have impeded our understanding of this family of transcriptional regulators. To date, 7 full-length LTTR structures have been published: CbnR (Muraoka et al., 2003), DntR (Smirnova et al., 2004), CrgA (Sainsbury et al., 2009), TsaR (Monferrer et al., 2010), BenM (Ruangprasert et al., 2010), ArgP (Zhou et al., 2010), and AphB (Taylor et al., 2012), with an additional two putative LTTRs from *P. aeruginosa* strains PA01 (PDB code 3FVZ) and PA0477

(PDB code 2ESN). At least 20 truncated versions of LTTRs without the DBD have also been deposited into the PDB. The presence of ions in the co-inducer binding sites, however, complicates our understanding of LTTR function. Ion bound structures may mimic the effect of the natural co-inducer molecule as observed in CysB (Tyrrell et al., 1997). Also, Ezezika and colleagues (2007a; 2007b) report that R156H variants of BenM (Ezezika et al., 2007a) and CatM (Ezezika et al., 2006) are transcriptionally active even in the absence of co-inducers, but full-length structural analysis of the BenM variant R156H showed no obvious conformational differences when compared to the wild-type protein structure (Ruangprasert et al., 2010). It is still not clear how co-inducer molecules affect the conformation of LTTRs, and in turn control gene expression. The lack of structural information continues to hamper our understanding of the LTTR family. Without structural information showing the binding of DNA by LTTRs, along with the interaction of co-inducer molecules, RNA polymerase, and other transcription factors, it is difficult to develop any unified model to describe LTTR regulation.

Thesis objectives

PtrA has been identified as a member of the LTTR family and an essential regulator of PA23 biological control activity. At present, very little is known about the PtrA protein and its control over gene expression. Therefore, the objectives of this thesis are as follows:

1. To characterize the structure using x-ray crystallography
2. To identify cognate binding sites within its own promoter

This information will shed light on the role of PtrA within the overall regulatory cascade of secondary metabolite production, and ultimately improve our understanding and ability to optimize *P. chlororaphis* PA23 as a biological control agent. Additionally, anything learned from PtrA will add further insight to the overall understanding of the LTTR family.

2. MATERIALS AND METHODS

2. 1. Biochemical and common reagents

Unless otherwise stated, all biochemicals and common reagents were purchased from Fisher Scientific Ltd. (Mississauga, ON, Canada) or Sigma-Aldrich Chemical Co. (St. Louis, MO, USA). Media components were purchased from Difco Laboratories (Detroit, MI, USA) or EMD Chemicals (Darmstadt, Germany). All growth media and aqueous solutions were prepared using MilliQ water (Millipore Co., Billerica, MA, USA).

2. 2. Bacterial strains and plasmids

The bacterial strains and plasmids used in this study are listed in Table 2.1 and Table 2.2, respectively. *E. coli* DH5α was used as a host strain for plasmid propagation and isolation. *E. coli* MT617 was used as a helper strain for tri-parental matings. *E. coli* BL21-Gold(DE3) and *E. coli* Rosetta^{TM}(DE3) were used as host strains for recombinant protein expression.

2. 2. 1. Media and growth conditions

E. coli cultures were grown at 37°C in Luria-Bertani Broth (LB; 10 g/L tryptone, 5 g/L yeast extract, and 5 g/L NaCl) or on LB agar solidified through the addition of 12 g/L agar. Test tube cultures were incubated on a TC-7 rotor (New Brunswick Scientific Co., NJ, USA). Cultures larger than 5 mL were grown in Pyrex fluted flasks and shaken at 180 rpm in a C-25 incubator shaker (New Brunswick Scientific Co., NJ, USA). *E. coli*

Table 2-1. Bacterial strains used in this study

Strain	Genotype or strain description	Source
Escherichia coli		
DH5α	*supE44* Δ*lacU169 (φ80 lacZ*ΔM15*) hsdR17 recA1 endA1 gyrA96 thi-1 relA1*	Gibco
MT607	*pro-82 thi-1 hsdR17 supE44 endA1 recA56*	Finan et al., 1986
MT616	MT607(pRK600) Cam^R	Finan et al., 1986
BL21-Gold(DE3)	F^- *ompT lon hsdSB*(r_B^- m_B^-) *gal dcm* λ(DE3)	Stratagene
Rosetta™(DE3)	F^- *ompT lon hsdS*$_B$(r_B^- m_B^-) *gal dcm* λ(DE3) pRARE (Cam^R)	Novagen
Pseudomonas chlororaphis		
PA23	Phz^+ Rif^R wild-type (soy bean plant isolate)	Savchuk and Fernando, 2004
PA23-443	*ptrA*::Tn5-OT182 genomic fusion (Tet^R, Amp^R)	Poritsanos, 2005

Table 2-2. Plasmids used in this study

Plasmid	Description	Source
pRK600	pRK2013 *npt*::Tn9 (Cam^R, Nm^R, Kan^R)	Finan et al., 1986
pSK+ (pBluescript™ II)	Cloning vector (ColE1 *oriV*, Amp^R)	Stratagene
pGS614	pSK+ inserted with 614 bp upstream of translational start site (ATG) of *ptrA* (Amp^R)	This study
pCR2.1TOPO	Cloning vector for PCR products (Amp^R)	Invitrogen
pTOPO-1.3kb*ptrA*	618 bp upstream and 676 bp downstream from translational start site (ATG) of *ptrA* cloned into pCR2.1TOPO (Amp^R)	Selin and de Kievit, unpublished
pTOPO-T11A	pTOPO-1.3kb*ptrA* containing mutated T-N_{11}-A LTTR binding region in *ptrA* promoter (Amp^R)	This study
pUCP23-*ptrA*	pUCP23 broad-host-range vector containing *ptrA* gene from *P. chlororaphis* PA23 (Amp^R Gm^R)	Selin and de Kievit, unpublished
pLP170	Promoterless *lacZ* transcriptional fusion vector (Amp^R)	Preston et al., 1997
pLP170-ptrA	pLP170 containing 1,297-bp *Xho*I-*Hin*d111 insert from pTOPO-1.3kb*ptrA* (Amp^R)	Selin and de Kievit, unpublished
pLP170-40	pLP170 containing 40 bp upstream and 676 bp downstream from translational start site (ATG) of *ptrA* gene (Amp^R)	This study
pLP170-52	pLP170 containing 52 bp upstream and 676 bp downstream from translational start site (ATG) of *ptrA* gene (Amp^R)	This study

pLP170-198	pLP170 containing 19 bp upstream and 676 bp downstream from translational start site (ATG) of *ptrA* gene (Amp^R)	This study
pLP170-614	pLP170 containing 614 bp upstream and 676 bp downstream from translational start site (ATG) of *ptrA* gene (Amp^R)	This study
pLP170-T11A	pLP170 containing mutated T-N_{11}-A LTTR binding region in *ptrA* promoter (Amp^R)	This study
pET28	Modified pET28b vector: tagless vector with reduced multiple cloning site comprised of *Nde*1/*Spe*1/*Bam*H1 (Kan^R)	Novagen
pET28-ptrAFL-tagless	Modified pET28b encoding full-length *ptrA* gene lacking a purification tag from *P. chlororaphis* PA23 (Kan^R)	This study
pET28Cterm	Modified pET28b vector: C-terminal His-tag sequence with reduced multiple cloning site comprised of *Nde*1/*Spe*1/*Bam*H1 (Kan^R)	Novagen
pET28-ptrAFL	Modified pET28b containing full-length *ptrA* gene with a C-terminal 6xHis tag from *P. chlororaphis* PA23 (Kan^R)	This study
pET28-ptrAEBD	Modified pET28b containing residues 82-301 (EBD) of the *ptrA* gene with a C-terminal 6xHis tag from *P. chlororaphis* PA23 (Kan^R)	This study

storage cultures were made from log-phase cultures, resuspended in 15% glycerol (v/v), and stored at -70°C in 2 mL cryogenic vials (Fisher).

P. chlororaphis cultures were routinely grown at 28°C in LB or peptone tryptic soy broth (PTSB) consisting of 5% peptone and 0.25% tryptic soy broth, as well as LB agar or Difco™ Pseudomonas Isolation Agar (PIA). All liquid cultures in test tubes and flasks were shaken at 220 rpm. *P. chlororaphis* storage cultures were resuspended in 10% skim milk powder (w/v) instead of glycerol.

2. 2. 2. Antibiotic concentrations in growth media

Where appropriate, antibiotics were added to growth media at a concentration of 100 μg/mL ampicillin (Amp), 50 μg/mL kanamycin (Kan), 34 μg/mL chloramphenicol (Cam), 20 μg/mL gentamicin (Gm), and 40 μg/mL piperacillin (Pip). Amp, Kan, and Gm were purchased from Research Products International Corp. (Mt. Prospect, IL, USA). Pip and Cam were purchased from Sigma-Aldrich Chemical Co. (St. Louis, MO, USA). All antibiotics, with the exception of Cam dissolved in 95% ethanol, were dissolved in water, filter sterilized using 0.2 μM filters (Sarstedt, Germany), and stored at -20°C.

2. 3. DNA manipulation

2. 3. 1. Plasmid DNA isolation and purification

Rapid isolation of plasmid DNA was purified using QIAprep miniprep kits (Qiagen, Hilden, Germany). Cells containing plasmids were grown to stationary phase in 1.5-5.0 mL LB supplemented with the appropriate antibiotic and pelleted by centrifugation. DNA purification was achieved by using the supplied spin columns

embedded with a silica membrane after alkaline lysis and clearing of the bacterial lysate using the supplied kit components. Plasmids were eluted from the membrane in 50 µL of water for sequencing or electroporation. For all other purposes, plasmids were eluted in TE buffer (10 mM Tris, 1 mM EDTA, pH 7.5).

Isolation of plasmid DNA for screening purposes was performed according to Sambrook *et al.* (1989). Cultures containing plasmids were grown to stationary phase in 1.5-5.0 mL LB supplemented with the appropriate antibiotic and the cells were pelleted by centrifugation (5,000 x g). The bacterial pellet was resuspended in 200 µL of glucose-EDTA-RNase buffer (25 mM Tris, 1% glucose, 10 mM EDTA, pH 8.0, and 0.34 mg/mL RNase). Alkaline lysis of cells was achieved using 400 µL of a solution containing 1% sodium dodecyl sulphate (SDS) and 0.2 M NaOH and incubating for 5 minutes after gentle mixing. A 300-µL aliquot of 6.3 M ammonium acetate (pH 5.9), was added to the solution, which was then mixed and centrifuged twice at max speed using a table top centrifuge for 10 minutes to remove precipitates. The supernatant was transferred to a fresh centrifuge tube and plasmid DNA was precipitated through the addition of 550 µL of isopropanol with incubation on ice for 15 minutes. DNA was pelleted by centrifugation for 10 minutes, washed twice with ice-cold 70% ethanol, and dried under vacuum. The DNA pellet was resuspended in TE buffer. Plasmid DNA isolation from *P. chlororaphis* strains included an additional phenol, chloroform, and isoamyl alcohol (25:24:1) purification after the neutralization step with ammonium acetate.

2. 3. 2. PCR amplification

The primers used in this study are listed in Table 2.3. Primers were synthesized by Invitrogen (Burlington, ON, Canada) or Alpha DNA (Montreal, QC, Canada) and stored at -20°C at 40 pM concentration in water. Unless otherwise stated, PCR reaction mixtures consisted of 20 mM Tris pH 8.4, 50 mM KCl, 0.2 mM dNTPs, 1.5 mM $MgCl_2$, 5% DMSO, 0.5 µM of each primer, 1-100 ng of template DNA, 2 units of *Taq* or *Pfu* DNA polymerase (prepared by Jack Switala, Department of Microbiology, University of Manitoba), and water to a final volume of 25 µL. A Px2 Thermal Cycler (Thermo Electron Corp, USA) was used for PCR amplifications and the reactions involved the following steps:

1. 94°C for 3 minutes
2. 94°C for 1 minute
3. 50-61°C (gradient) for 1 minute
4. 72°C for 1 minute
5. Steps 2-4 repeated 25 times
6. 72°C for 10 minutes
7. Hold at 4°C

All PCR reactions were performed using pUCP-ptrA as template DNA and the amplification conditions listed above. Mutating the hypothesized T-N_{11}-A box within the *ptrA* promoter region was achieved by amplifying the entire pTOPO-1.3kb*ptrA* plasmid (Table 2.2) using 5′ phosphorylated primers harbouring the mutation. The resulting 5.2-kb PCR product was generated using *Pfu* DNA polymerase and an extension time of 10 minutes instead of 1 minute (step 4).

Table 2-3. Oligonucleotide primers used for PCR amplification in this study

Primer name[f]	Primer sequence (5′ – 3′)	Restriction site	Use
PtrA-F	GTGGGC**CATATG**GATGACCTGGCGGCG	*Nde*1	C-6xHis and tagless PtrA forward primer
EBD-F	CGCCAG**CATATG**GCGCGGCTCAAGGAC	*Nde*1	PtrA-EBD forward primer
PtrA-R	GATATAAAG**GGATCC**GAGGCGATCCA GCGC	*Bam*H1	Reverse primer
40-F	GCGCAC**GAATTC**GCAACCTTTGGT	*Eco*R1	Forward primers for promoter truncations
52-F	TCCCGT**GAATTC**GCGCACTTATAG	*Eco*R1	
198-F	GGC**GAATTC**GGATGATTTCATGACG	*Eco*R1	
614-F	CAC**GAATTC**ACGGGGCGTAACTGTC	*Eco*R1	
ATG-R	GCG**GGATCC**AGGTCATCCATCT	*Bam*H1	Reverse primer for gel shift assays
676-R	AGC**GGATCC**TTTTTCAGCAGGTT	*Bam*H1	Reverse primer for generating transcriptional fusions
T11A-F	[a]P_CGACAACTGGAACCAATCCGTGGGC GAGAT	-	Primer pair for mutating hypothesized $T\text{-}N_{11}\text{-}A$ box
T11A-R	[a]P_ACCAAAGGTTGCCTATTAGTGCGCT AA	-	

[a] "P_" indicates a phosphorylated primer at the 5′ end

2. 3. 3. DNA concentration determination

Samples containing DNA were typically diluted 100-fold in water and measured spectrophotometrically (Ultrospec 3100 pro, GE Healthcare, Canada) in a 1.4 mL Hellma 104-QS quartz cuvette (Fisher). An A_{260} reading of 1.0 was considered to be equivalent to 50 µg/mL of double-stranded DNA. Therefore, the unknown DNA sample concentration was calculated using the following formula:

[DNA] (µg/mL) = 50 µg/mL x A_{260} x dilution factor

2. 3. 4. Restriction endonuclease digestion of DNA

All restriction enzymes were purchased from Invitrogen and restriction digests were carried out according to the supplied protocols. Reactions were allowed to proceed for a minimum of 2 hours at 37°C. Double digests of DNA using two different restriction enzymes were performed simultaneously if a suitable buffer was recommended by Invitrogen. Otherwise, ethanol precipitation of DNA was carried out prior to the addition of the second restriction enzyme.

2. 3. 5. Agarose gel electrophoresis

Electrophoresis of PCR-amplified DNA, restriction endonuclease-digested DNA, or plasmid DNA was performed according to Sambrook *et al*. (1989). Using 1% agarose gels in TAE buffer (40 mM Tris-acetate, 1 mM EDTA, pH 8.0), DNA samples were mixed with a 1:10 dilution of 10X Loading Buffer (Invitrogen) which contained 1% SDS, 50% glycerol, and 0.05% Bromophenol blue before loading into the wells. A 1 Kb Plus™ DNA ladder (Invitrogen) was run in parallel as size standards. Electrophoresis

was performed at a constant voltage of 100V and stopped when the blue dye migrated approximately two-thirds down the length of the gel. DNA was stained with ethidium bromide, visualized with UV light, and imaged using a Gel Doc 1000 image capture (Bio-Rad).

2. 3. 6. Gel purification of DNA

DNA separated by agarose gel electrophoresis was purified using an UltraClean™ 15 DNA purification kit (Mo Bio Laboratories Inc., CA, USA) according to the manufacturer's protocol. Briefly, the excised DNA fragment in the agarose gel was melted in sodium iodide at 55°C and 6-10 µL of glass milk was added to the solution and mixed. After a minimum of 5 minutes, the glass milk was pelleted by centrifugation and washed with the provided wash buffer. The glass milk was pelleted twice to remove all traces of wash solution by aspiration. The pellet was dried for 5 minutes under vacuum and then resuspended in 10-20 µL of TE buffer to recover DNA.

2. 3. 7. Ligation

T4 DNA ligase supplied with 5X ligation buffer was purchased from Invitrogen. Restriction endonuclease-digested insert and plasmid were ligated together according to Sambrook *et al*. (1989). Purified DNA fragments were ligated in reaction volumes of 10-20 µL and allowed to incubate at 15°C overnight.

2. 3. 8. Transformation

E. coli cells were grown to early-log phase (OD_{600} of 0.3-0.5) in LB. Cells were pelleted by centrifugation and resuspended with ice-cold 0.1 M $CaCl_2$ or ice-cold TSS (10% w/v PEG-6000, 5% v/v DMSO, 50 mM $MgSO_4$ in LB) in 1/20th of the original culture volume. The cells were incubated on ice for a minimum of 30 minutes. Plasmid DNA was then added to 100 µL of $CaCl_2$-competent cells or TSS-competent cells, incubated on ice for an additional 30 minutes, and heat-shocked for 90 seconds at 42°C. Cells were transferred back on ice for 2-5 minutes. 1 mL of LB was added and bacteria were incubated for 1 hour at 37°C. The cells were then spread onto selective media and grown overnight. Single colonies were plated and screened by plasmid isolation and restriction digest, followed by sequence analysis.

2. 3. 9. Tri-parental mating

Mobilizing plasmids into *P. chlororaphis* cells was achieved by tri-parental matings using *E. coli* DH5α as the donor strain containing the plasmid of interest and *E. coli* MT617 as the helper strain harbouring pRK600. The three strains, donor, helper, and recipient, were grown separately on solid media containing the appropriate antibiotics. Approximately equal amounts of bacteria were picked from each plate using an applicator stick (Fisher) and resuspended in 1.5 mL of LB. The cells were washed once with an equal volume of LB, resuspended in 50 µL of LB, and spotted onto LB agar containing 10 mM $MgSO_4$. After overnight incubation at 28°C, the cells were scraped from the plate and washed twice with 1x PBS (pH 7.4). Serial dilutions were plated onto

PIA containing 200 µg/mL Pip. Single colonies were picked and screened by plasmid isolation and restriction digest to identify plasmids with the correct DNA insert.

2. 3. 10. Electroporation

P. chlororaphis strains were rendered electrocompetent by a series of sucrose washes at 4°C. Cells were grown to an OD_{600} of 0.5, pelleted by centrifugation, and washed three times with 300 mM sucrose. Cells were resuspended in 300 mM sucrose at 1/500th the original culture volume. Electrocompetent cells were aliquoted into 40 µL volumes and stored at -70°C.

Electrocompetent cells, after being thawed on ice, were mixed with 2 µL of plasmid DNA. The cells were transferred to a 1 mm gap, 90 µL electroporation cuvette (Fisher) and placed back on ice. A BTX Electro Cell Manipulator™ 600 (Genetronics Inc., CA, USA) was used at 1.6 kV with a resistance timing of 129 ohms. After electroporation, 1 mL of LB was added to the cells which were then allowed to shake for 2 hours at 28°C before spreading onto selective media for overnight growth. Single colonies were patch plated and screened by plasmid isolation and restriction digest to identify plasmids with the correct DNA insert.

2. 3. 11. DNA sequencing

DNA sequence analysis was performed using an Applied Biosystem 3130 Genetic Analyzer (Life Technologies Corp., Carlsbad, CA, USA) supplied software (3130 Data Collection v3.0 and Autoanalysis Manager 3.0). Each sequencing reaction mixture contained 150-300 ng of DNA, 3.2 pM sequencing primer, 0.5 µL BigDye® Terminator

v3.1 (Applied Biosystems) and 2 µL 5x Sequencing Buffer (Applied Biosystems) brought up to a final volume of 20 µL with water. The PCR cycle using a Px2 Thermal Cycler (Thermo Electron Corp) involved the following steps:

1. 96°C for 1 minute
2. 96°C for 10 seconds
3. 50°C for 5 seconds
4. 64°C for 4 minutes
5. Steps 2-4 repeated 25 times or repeated 99 times if performed overnight
6. Hold at 4°C

The DNA was then treated with 2 µL of 125 mM EDTA (pH 8.0), 2 µL of 3 M sodium acetate (pH 4.8), and 60 µL of 95% ice-cold ethanol. After mixing by inversion followed by 15 minutes of incubation at room temperature, the DNA was pelleted at maximum speed in a table-top centrifuge at 4°C for 15 minutes. The supernatant was aspirated and the DNA pellet was washed twice with 70% ice-cold ethanol before drying under vacuum. The purified DNA was then denatured with 20 µL Hi-Di^{TM} formamide (Applied Biosystems) at 94°C for 5 minutes. A 19-µL aliquot of the sequencing reaction was used for sequence analysis.

2. 4. Cloning of full-length PtrA, the PtrA effector binding domain, and the *ptrA* promoter region from *P. chlororaphis* PA23

2. 4. 1. Construction of C-terminal 6xHis and tagless PtrA over-expression plasmids

The gene encoding PtrA was PCR amplified from pUCP23-*ptrA* as template DNA using the primers PtrA-F and PtrA-R (Table 2.3). The PCR product was digested with *Nde*1 and *Bam*H1 and ligated into a modified pET28Cterm vector (Table 2.2). The resulting plasmid construct adds additional nucleotides to the C-terminus, which incorporates a Gly-Ser-His-His-His-His-His-His tag at the C-terminus of the protein. The

PCR product was also ligated into a modified version of pET28 vector (Table 2.2) containing the same reduced multicloning site (*Nde*1/*Spe*1/*Bam*H1) but lacking an affinity purification tag. The stop codon is located within the plasmid, resulting in the addition of nucleotides from the *Bam*H1 restriction site (GGATCC), which incorporates two additional amino acid residues (GS) at the C-terminus of the protein. The ligated products were used to transform *E. coli* DH5α cells. The resulting plasmids pET28-ptrAFL and pET28-ptrAFL-tagless (Table 2.2) were isolated from a two-Amp resistant transformants. Restriction analysis and DNA sequencing were performed to verify the plasmid constructs, which were then transformed into *E. coli* Rosetta^{TM}(DE3) cells.

2. 4. 2. Construction of a PtrA effector-binding domain over-expression plasmid

The DNA binding domain of PtrA was removed by PCR amplifying a truncated version of the gene using the primers EBD-F and PtrA-R (Table 2.3) and pUCP23-*ptrA* as template DNA. The PCR product and the modified pET28Cterm vector (Table 2.2) were digested with *Nde*1 and *Bam*H1 and ligated together. The resulting plasmid construct adds additional nucleotides to the C-terminus, which translates into a GSHHHHHH amino acid sequence, prior to the stop codon. The ligation product was transformed into *E. coli* BL21-Gold(DE3) cells. The resulting plasmid pET28-ptrAEBD (Table 2.2) was isolated from a single Kan resistant transformant and verified by restriction analysis and DNA sequencing.

2. 4. 3. Generation of *ptrA* truncated promoter constructs

PCR primers 40-F, 52-F, 198-F, 614-F, ATG-R, and 676-R (Table 2.3) were used to generate full-length and truncated versions of the *ptrA* promoter region for electrophoretic mobility shift assays (EMSAs) and β-galactosidase assays. pUCP23-*ptrA* was used as template DNA. The PCR products were digested with *Eco*R1 and *Bam*H1 and ligated into pSK+ and pLP170 (Table 2.2). Mutation of the hypothesized T-N_{11}-A region involved incorporating the mutation within the pTOPO-1.3kb*ptrA* plasmid using primers T11A-F and T11A-R (Table 2.3) and PCR amplifying the entire plasmid (section 2. 3. 2.). The PCR product was ligated and transformed into *E. coli* DH5α. The plasmid containing the mutation, pTOPO-T11A, was verified by DNA sequencing before the insert was removed as a 1.3-kb *Xho*1/*Hin*d111 fragment and ligated into the same sites of pLP170. The resulting plasmid constructs pLP170-40, pLP170-52, pLP170-198, pLP170-614, and pLP170-T11A (Table 2.2) were transformed into *E. coli* DH5α and verified by restriction analysis and DNA sequencing. The plasmids were then mated or electroporated into *P. chlororaphis* PA23 and verified by restriction analysis.

2. 5. Recombinant protein purification

2. 5. 1. Small-scale optimization of protein expression

Initial experiments designed to optimize protein expression were performed using 30 mL culture volumes in Pyrex fluted flasks by varying the following parameters: the point of induction (OD_{600}), IPTG concentration, induction duration, and induction temperature. Plasmid-carrying *E. coli* BL21-Gold(DE3) and *E. coli* Rosetta™(DE3) cells were grown initially at 37°C with shaking until cells reached early or late log-phase

with OD_{600} between 0.3-1.5. A low or high concentration of IPTG (0.1 mM and 1.0 mM) was then added, and the cells were further incubated with shaking between 2-16 hours at varying temperatures (RT, 28°C, and 37°C).

Recombinant protein expression levels were analyzed by SDS-PAGE. Whole cell protein expression was analyzed by first diluting an aliquot of culture to an OD_{600}. A 5-µL aliquot of a 20-fold concentrated resuspension of cells in lysis buffer was analyzed by SDS-PAGE. Soluble and insoluble protein fractions were also analyzed by disrupting the remainder of the cells in lysis buffer using a sonicator (Fisher sonic dismembrator model 300, Artek System Corp.) and centrifuging the samples for 10 minutes at max speed in a tabletop centrifuge prior to electrophoresis.

2. 5. 2. Large scale protein overexpression and cell lysis by French press

Large scale purification was achieved by growing 0.5 L cultures in Pyrex fluted flasks with shaking following the optimized parameters for recombinant protein expression (section 2. 5. 1.). Cells were harvested by centrifugation at 7,000 rpm for 10 minutes using a Sorvall GS-3 rotor (Thermo Scientific) and frozen as a dry pellet at -70°C. Cells were thawed and resuspended in ice-cold lysis buffer at a ratio of 7.5 mL buffer to 1 g of cells. The cells were lysed by French Press (American Instrument Company, MD, USA) in a chilled 20,000 psi limit cell with a single pass at 12,000 psi. Cell lysate was centrifuged (17,000 x g) at 4°C for a minimum of 30 minutes, yielding the crude extract.

2. 5. 3. Streptomycin sulfate precipitation of nucleic acids

Streptomycin sulfate was added slowly, with stirring, to a final concentration of 2.5% (w/v) to the crude extract obtained after French press. The solution was stirred for a minimum of 20 minutes. The nucleic acids were separated by centrifugation (17,000 x g) for 20 minutes.

2. 5. 4. Polyethyleneimine precipitation of nucleic acids

A 5% (w/v) polyethyleneimine (PEI) working solution was prepared from a 50% PEI (w/v) stock solution. The PEI working solution was adjusted to pH 7.9 using HCl and then filtered through a 0.2 µm regenerated cellulose filter (Sartorius Stedim Biotech, Germany) and stored at 4°C. Precipitation of nucleic acids was achieved by adding the PEI working solution drop-wise, with stirring, to a final concentration of 0.15% (w/v). The solution was stirred for a minimum of 20 minutes prior to centrifugation.

2. 5. 5. Ammonium sulfate precipitation

Ammonium sulfate was added slowly at room temperature, with stirring, starting at a 30% saturation of ammonium sulfate based on a 4.1 M saturation of ammonium sulfate at 25°C. The Ammonium Sulfate Table by Green and Hughes (1955) was used to determine the amount of ammonium sulfate to add in order to achieve higher percentage saturations at increments of 10%. After the addition of ammonium sulfate, the solution was stirred for 20 minutes and then centrifuged (17,000 x g) for 30 minutes. The pellet obtained from each ammonium sulfate cut was resuspended in lysis buffer and analyzed by SDS-PAGE for the desired protein. The ammonium sulfate cut containing the desired

protein was dialyzed in a suitable chromatography buffer using 12,000-14,000 MWCO regenerated cellulose dialysis tubing (Fisher).

2. 5. 6. DNAse I treatment

A 5 mg/mL stock solution of DNase I from bovine pancrease (Sigma) was prepared in 20 mM sodium acetate, 0.1 mM phenylmethanesulfonylfluoride, 5 mM $CaCl_2$, and 50% (v/v) glycerol (pH 6.5). It was added to a final concentration of 10-50 µg/mL, along with 1-10 mM $MgCl_2$, to lysis buffers prior to French Press or purified protein samples. Reaction mixtures were incubated for a minimum of 30 minutes at three different temperatures (4°C, RT, and 37°C).

2. 5. 7. Purification of full-length PtrA

2. 5. 7. 1. Immobilized metal-ion affinity chromatography

E. coli Rosetta^{TM}(DE3) cells harbouring pET28-ptrAFL were grown to an OD_{600} of 0.7 at 37°C. The cells were induced with 0.1 mM IPTG for 16 hours at 28°C with shaking at 180 rpm. After harvesting the cells (section 2. 5. 2.), the cells were lysed in TNG lysis buffer (50 mM Tris, 500 mM NaCl, 10% glycerol, pH 7.5). The cell lysate obtained after French press was centrifuged (17,000 x g) for 1 hour and directly loaded onto a Ni-NTA column. Purification was performed using a step-wise gradient following the manufacturer's recommendation (Qiagen). The column was washed with TNG buffer supplemented with 0, 50 and 150 mM imidazole before eluting bound protein with 500 mM imidazole.

2. 5. 7. 2. Denaturation and refolding of full-length PtrA

E. coli Rosetta™(DE3) cells harbouring pET28-ptrAFL (Table 2.2) were grown to an OD_{600} of 0.7 at 37°C in Terrific Broth (12 g/L tryptone, 24 g/L yeast extract, 0.5% glycerol, 2.312 g/L KH_2PO_4, and 12.541 g/L K_2HPO_4). The cells were induced with 0.1 mM IPTG for 16 hours at 37°C with shaking at 180 rpm. The cells were harvested (section 2. 5. 2.), but lysed with multiple passages through the French Press in TN buffer (20 mM Tris, 500 mM NaCl, pH 7.5). The heat generated from multiple passages through the French Press caused the recombinant protein to fractionate into the pellet after centrifugation (17,000 x g) for 30 minutes.

The pellet was washed twice with TN buffer with 1% Triton X-100 and another wash step without Triton X-100, followed by two more washes with TN buffer containing 1% *n*-dodecyl β-D-maltoside. Prior to solubilising the pellet in 8 M urea or 6 M guanidine hydrochloride in TN buffer supplemented with 1 mM TCEP, the pellet was washed once more with TN buffer. The pellet was incubated with the solubilisation buffer for 1 hour with shaking before centrifugation. Refolding of PtrA was attempted by a decreasing step-wise gradient of denaturing agents either by dialysis or on column.

2. 5. 7. 3. Streptomycin sulfate and PEI precipitation of nucleic acids and resolubilisation of PtrA

E. coli Rosetta™(DE3) cells harbouring pET28-ptrAFL-tagless (Table 2.2) were grown to an OD_{600} of 0.7 at 37°C. The cells were induced with 0.1 mM IPTG for 16 hours at 28°C with shaking at 180 rpm. After harvesting the cells (section 2. 5. 2.), they were lysed in 50 mM Tris, 100 mM NaCl, 0.1 mM EDTA, and 0.1 mM TCEP (pH 7.9).

PEI precipitation (section 2. 5. 4.) and streptomycin sulfate precipitation (section 2. 5. 3.) were performed on separate samples. Nucleic acids and PtrA protein were pelleted by centrifugation (5,000 x g). The pellet was washed once more in lysis buffer before eluting the protein bound to DNA with a higher concentration of NaCl at 0.5 M. The solution was centrifuged (17,000 x g) for 20 minutes. Ammonium sulfate was added to the supernatant at 60% saturation in order to remove PEI from solution. The ammonium sulfate precipitated protein was dialyzed against a suitable chromatography buffer for further purification.

2. 5. 7. 4. Heparin column

Purification using a 1 mL HiTrap Heparin HP column (GE Healthcare) was also attempted. All protein solutions were first dialyzed against heparin binding buffer (50 mM Tris, 150 mM NaCl, 0.1 mM EDTA, and 10% glycerol, pH 8.0) and filtered through 0.2 µm filters (Fisher) before sample loading on the syringe-operated column. Purification was performed using a step-wise gradient involving 5 column volumes per step ranging from 0.15 – 2.0 M NaCl.

2. 5. 8. Purification of the PtrA effector-binding domain

2. 5. 8. 1. Streptomycin sulfate precipitation followed by immobilized metal-ion affinity chromatography

E. coli BL21-Gold(DE3) cells harbouring pET28-ptrAEBD were grown to an OD_{600} of 0.7 at 37°C. The cells were induced with 0.1 mM IPTG for 16 hours at 37°C with shaking at 180 rpm. After harvesting the cells (section 2. 5. 2.), the cells were lysed

in TNIT buffer (50 mM Tris, 500 mM NaCl, 40 mM imidazole, 1 mM TCEP, pH 8). All of the steps from this point on were performed at room temperature. The crude extract was treated with ammonium sulfate (section 2. 5. 5.). PtrA-EBD precipitated out in the first ammonium sulfate cut of 30% saturation. The pellet was resuspended and dialyzed against 3 buffer exchanges of fresh TNIT buffer, with a minimum 200-fold excess volume, over the course of 6 hours. The dialyzed protein solution was centrifuged (13,000 x g) for 10 minutes and loaded directly onto a 5-mL gravity Ni-NTA column (Qiagen). The column was washed with 5 column volumes of TNIT buffer containing 0 and 150 mM imidazole and then eluting PtrA-EBD with TNIT buffer containing 350 mM imidazole.

The eluted PtrA-EBD protein solution was dialyzed several times against a buffer containing 10 mM Tris, 500 mM NaCl, and 1 mM DTT (pH 8.0) with a minimum 200-fold excess volume for 4 hours per buffer exchange. A final buffer exchange against a 10 mM Tris, 500 mM NaCl, and 1 mM TCEP (pH 8.0) buffer and concentration step was performed under nitrogen gas in a Amicon 8050 stirred pressure cell (Millipore, USA) using a YM-30 ultrafiltration membrane (Millipore, USA) with a molecular weight cut-off (MWCO) of 30 kDa. If required, purified PtrA-EBD was further concentrated using an Amicon Ultra centrifugal filter (Millipore, USA) with a MWCO of 10 kDa.

2. 5. 8. 2. Denaturing and refolding purified PtrA-EBD in the presence of reducing agents

Purified PtrA-EBD was denatured with urea to a final concentration of 8 M in 10 mM Tris, 500 mM NaCl, and 1 mM TCEP (pH 8.0). The urea-denatured protein was

refolded by dialysis against a decreasing step-wise gradient of 6, 4, 2 and 0 M urea in a buffer containing 10 mM Tris, 500 mM NaCl, and 13 mM β-mercaptoethanol (pH 8.0). A minimum of a 100-fold excess buffer volume for 2 hours per buffer exchange was used. A final buffer exchange against a 10 mM Tris, 500 mM NaCl, and 1 mM TCEP (pH 8.0) buffer and concentration step was performed under nitrogen gas in the Amicon 8050 stirred pressure cell (Millipore) as described above (section 2. 5. 7. 1.).

2. 6. Protein purification analysis

2. 6. 1. Protein concentration determination

2. 6. 1. 1. Protein purity estimation (A_{280}/A_{260})

Rapid estimation of protein concentration was done spectrophotometrically (Ultrospec 3100 pro) using the Warburg-Christian method (Warburg and Christian, 1941; Layne, 1957). Typically, protein samples were diluted 100-fold and placed in a quartz cuvette (Fisher). The unknown protein concentration was estimated using the following formula:

[Protein] (mg/mL) = (1.55 × A280) – (0.76 × A260) x dilution factor

2. 6. 1. 2. Bradford assay

All Bradford assays were performed using protein assay dye reagent concentrate (Bio-Rad). Measurements were taken from 1-mL volumes consisting of 200 µL of protein dye added to 800 µL of diluted protein sample. A bovine serum albumin stock solution (2 mg/mL) was diluted to create a linear standard curve of 0, 1.25, 2.5, 5.0, and 10 µg/mL. After the addition of protein dye reagent, samples were vortexed and

incubated for approximately 5 minutes prior to measuring the absorbance at 595 nm using an Ultrospec 3100 pro (GE Healthcare). Absorbance values were only accepted if values were within the linear range corresponding to 1.0 and 10.0 µg/mL of protein.

2. 6. 1. 3. Extinction coefficient

Purified protein concentrations of PtrA-EBD were measured using the extinction coefficient method. The extinction coefficient (ε) for PtrA-EBD was determined to be 35,870 M^{-1} cm^{-1} using ProtParam tool from the ExPASy online server (Gasteiger et al., 2003; Gasteiger et al., 2005). Absorbance readings at 280 nm were measured using a Nanodrop 2000c spectrophotometer (Thermo Scientific, Ottawa, ON) and the sample protein concentration was calculated using the Beer-Lambert Law equation:

Absorbance = ε (L/mol x cm) x concentration (mol/L) x cell length (cm)

2. 6. 2. Reducing and non-reducing SDS-PAGE

Sample preparation and SDS-polyacrylamide electrophoresis to assess protein overexpression and purification were performed according to Laemmli (1970). All gels were cast in 10 mm x 10 mm x 0.75 mm glass plates using 10 or 15 well combs, consisting of a 5% stacking gel and 12% separating gel.

Protein concentrations were determined to ensure equal amounts of protein (2-8 µg) were loaded per lane. Protein samples were mixed with an equal volume of reducing and denaturing sample buffer (3.4 mg/mL NaH_2PO_4, 10.2 mg/mL Na_2HPO_4, 10 mg/mL SDS, 13 mM 2-mercaptoethanol, and 0.36 g/mL urea) and boiled for a minimum of 3 minutes with an additional 20% volume of 1% bromophenol blue. Non-reducing SDS-

PAGE did not contain 2-mercaptoethanol in the sample buffer. Benchmark™ ladder (Invitrogen) was used as a reference for molecular weight determination. Gels were run at a constant voltage of 150 V in a Tris-glycine running buffer (14 g/L glycine, 3 g/L Tris and 1 g/L SDS). Gels were stained (0.5 g/L Coomassie Brilliant Blue R-250, 30% methanol, and 10% acetic acid) for a minimum of 30 minutes, destained (15% methanol and 7% acetic acid) until the background was clear, and then subjected to a final destain (7% acetic acid and 1% glycerol) for a minimum of 1 hour prior to gel drying. Gels were dried on 0.16 mM Whatman paper (W & R Balston Ltd., England) covered with cellophane membrane backing (Bio-Rad), and dried at 80°C for a minimum of 1 hour on a Savant SGD4050 slab gel drier (Thermo Scientific) under vacuum.

2. 6. 3. Native PAGE

All non-denaturing polyacrylamide gel electrophoresis was performed in the absence of SDS. Gels were cast and run following a protocol similar to the denaturing PAGE method described above (section 2. 6. 2.). A 4% Tris stacking gel (pH 6.8) and 8% Tris separating gel (pH 8.8) were used for protein separation, and a 5% TBE gel (89 mM Tris-borate, 2 mM EDTA, 5% acrylamide, 0.2% bisacrylamide, 0.5 mg/mL ammonium persulfate, 5 µL TEMED) was used for EMSAs.

Gels were typically run at a constant voltage of 50 V in a Tris-borate-EDTA running buffer (108 g/L Tris, 55 g/L boric acid, 9.3 g/L EDTA, pH 8.3) or Tris-glycine running buffer (28.8 g/L Tris, 6.0 g/L glycine). Protein staining and destaining was performed as described above (section 2. 6. 2.). DNA was stained using a 10,000-fold dilution of SYBR® Green I in ddH_2O for 10 minutes with shaking, followed by two

rinses with ddH_2O. DNA bands were imaged using AlphaImager® EP (Cell Biosciences, Inc., USA).

2. 6. 4. Dynamic light scattering

All measurements were performed using the Nano-S Dynamic Light Scattering system (Malvern Instruments Ltd., Malvern, UK) that has a 633-nm laser and a scattering angle of 173°. Samples were analyzed in a 45-µL quartz cuvette (Fisher). Samples were allowed to equilibrate for 3 min at 20°C before collecting the data in "automatic mode". Five separate measurements were made. The resulting data were analysed using DTS software Version 6.00 (Malvern Instruments Ltd., Malvern, UK).

2. 6. 5. Analytical gel filtration chromatography

Between 1-2 mg of purified PtrA-EBD in a volume of 200 µL was injected onto a Superdex™ 75 10/300 GL gel filtration column (GE Healthcare). A constant flow rate of 0.3 mL/min, controlled by an ÄKTA-FPLC (GE Healthcare) with continuous UV absorption (A_{280}) detection of column effluent and automated fraction collection, was performed at room temperature. The gel filtration buffer containing 10 mM Tris, 500 mM NaCl, and 1 mM TCEP (pH 8.0) was degassed prior to use.

2. 6. 6. Mass spectrometry

Purified PtrA-EBD was given to Dr. Lynda J. Donald (Department of Chemistry, University of Manitoba) for mass spectrometry (MS) analysis. The protein samples were dialyzed overnight at room temperature against a 0.5 M ammonium bicarbonate and 1

mM DTT buffer using Pierce Slide-A-Lyzer cassettes (Thermo Scientific). The protein was then diluted to ~1 µM (calculated based on the mass of a monomer) and 3-5 µL volumes were inserted into a New Objective^{TM} capillary and analyzed by nanospray ionization. For denaturing MS analysis using electrospray ionization, protein was denatured in 1% acetic acid and 50% methanol and diluted to ~10 µM. Precipitated protein on the dialysis membrane was also analyzed separately by denaturing MS. All MS experiments were analyzed using a modified time-of-flight mass spectrometer built in the Department of Physics & Astronomy, University of Manitoba (Kozlovski et al., 2005).

2. 7. β-galactosidase assays to determine promoter activity of *ptrA*

To monitor *ptrA* promoter activity, β-galactosidase analysis of transcriptional fusions was performed. Full-length and truncations of the *ptrA* promoter region were cloned into pLP170 and mobilized into PA23. The level of transcriptional activity was monitored by β-galactosidase activity. Cultures were grown in PTSB containing 5% peptone and 0.25% tryptic soy broth. Cultures were adjusted to an OD_{600} of 0.01 and incubated at 28°C with shaking until the desired time point or stationary phase was reached. Cells from 5 µL of culture were solubilised and incubated at 28°C using 0.01% SDS and 2% chloroform in Z-buffer (0.06 M $Na_2HPO_4 \cdot 7H_2O$, 0.04 M $NaH_2PO_4 \cdot H_2O$, 0.01 M KCl, 0.001 M $MgSO_4$, 0.05 M βME, pH 7.0) prior to the addition of 0.8 mg of ONPG to a total reaction volume of 1 mL. β-galactosidase activity was determined by measuring the hydrolysis of ONPG at A_{420} as described by Miller (1972). All assays were performed in triplicate.

2. 8. Protein crystallization

Initial protein crystallization trials were screened using 96-well NeXtal Deep-Well block cyrstallization screens purchased from Qiagen. Liquid-handling was performed using a Gryphon crystallization robot (Art Robbins Instruments, USA). Crystals were grown at room temperature using the sitting drop vapour diffusion method in 96-well Intelli-Plate^{TM} 3-well crystallography plates (Art Robbins Instruments). Wells contained 50 µL of reservoir crystallization mother liquor and drop sizes of 0.6 µL with a 1:1 ratio of protein solution to mother liquor. Optimization of crystallization conditions was performed in 24-well screw-cap NeXtal plates (Qiagen) containing 1 mL reservoir mother liquor and 2 µL hanging drops containing 1:1 ratio of protein solution to mother liquor.

3. RESULTS

3. 1. Purification of full-length PtrA

The initial goal of this research was to purify the full-length PtrA protein necessary for downstream DNA-binding assays and protein structural analysis. The insolubility issues encountered during protein purification thwarted attempts to obtain a concentrated protein sample ideal for protein crystallization. Electrophoretic mobility shift assays were also unsuccessful as purified PtrA failed to enter a native gel. The following section chronicles the purification strategies attempted for full-length PtrA.

3. 1. 1. Expression and purification of His-tagged PtrA

The *ptrA* gene, encoding a LysR-type transcriptional regulator of 301 amino acids in length, was cloned into a modified pET28b vector for protein overexpression. The plasmid construct added a His-tag to the C-terminal end of the protein. The recombinant PtrA protein was overexpressed in *E. coli* Rosetta cells harbouring pRARE, which compensated for any codon bias by providing tRNA genes that rarely occur in *E. coli*.

At the time of research, only 6 full-length LTTR structures were published—five of which were purified using a C-terminal His-tag (Smirnova et al., 2004; Sainsbury et al., 2008; Monferrer et al., 2008; Zhou et al., 2010; Ruangprasert et al., 2010). The same purification strategy of His-tagging the C-terminus was followed for PtrA. Unfortunately, purification of PtrA did not exhibit the same level of success compared to the LTTRs for which structures had been solved. Although the majority of overexpressed PtrA protein remained in the soluble fraction of the crude extract after cell lysis, the bulk

Table 3-1. Summary of the different binding buffers used to purify His-tagged PtrA using immobilized nickel-ion affinity chromatography.

	Buffer (50 mM)	pH	NaCl (M)	Other additives
1.	Tris	8	0.5	
2.	Tris	8	0.5	10% glycerol, 10 mM imidazole
3.	Tris	8	0.5	10% glycerol, 40 mM imidazole
4.	Tris	7	0.5	10% glycerol, 10 mM imidazole
5.	Tris	8.5	0.5	10% glycerol, 10 mM imidazole
6.	Tris	8	1.0	10% glycerol
7.[α]	Tris	8	0.5	20% glycerol, 10 mM imidazole
8.	Tris	8	2.0	10% glycerol, 10 mM imidazole
9.	Sodium phosphate	7.4	1.0	
10.	Sodium phosphate	7.4	0.5	0.2 mM PMSF, 10 mM $MgCl_2$, 20 µg/mL DNAse
11.	Tris	8	1.0	4.0 M urea, 10% glycerol, 10 mM imidazole
12.	Tris	8	0.5	10% glycerol, 0.2% Tween-20, 10 mM imidazole
13.	Tris	8	0.5	10% glycerol, 0.2% Tween-20, 10 mM imidazole, 4 mM βME
14.	Tris	8	0.5	10% glycerol, 0.2% Tween-20, 10 mM imidazole, 0.5 µg/mL DNAse, 1 mM $MgCl_2$
15.	Tris	8	0.5	10% glycerol, 0.2% Tween-20, 10 mM imidazole, 50 µg/mL DNAse, 10 mM $MgCl_2$
16.	Tris	8	0.5	10% glycerol, 10 mM imidazole, 10 mM NDSB-195
17.	Tris	8	0.5	10% glycerol, 10 mM imidazole, 10 mM NDSB-195, 4 mM βME
18.	Tris	7.5	0.5	8.0 M urea
19.	Tris	7.5	0.5	6.0 M guanidine hydrochloride

[α] A duplicate run was performed with an additional 2M NaCl binding buffer wash during purification

of the PtrA protein did not bind to the nickel column and ended up in the flow through (Figure 3-1). Incubating the crude extract with the Ni-NTA beads and loading the sample by batch method did not improve yield, nor did reloading the pooled flow-through fractions back onto the column. Varying the pH (7.0-8.5), glycerol (0-20%) and NaCl concentrations (0.5-2.0 M), and supplementing the lysis buffer with additives (imidazole, NDSB-195, Tween-20, and reducing agents) was also tried (Table 3-1). None of the aforementioned lysis buffers were successful in improving yield or purity. A yield of less than 0.5 mg of purified PtrA was obtained per litre of cell culture. Attempts to concentrate the sample beyond ~0.5 mg/mL were unsuccessful.

3. 1. 2. Association of PtrA with DNA

For the solved full-length structures of DntR (Smirnova et al., 2004) and TsaR (Monferrer et al., 2008), the authors noted the addition of DNAse during purification to improve both yield and purity. The same strategy was employed for PtrA. The addition of DNAse during cell lysis resulted in some precipitation of PtrA as judged by SDS-PAGE (Figure 3-2). Subsequent loading of crude extracts treated with DNAse onto the nickel column did not improve yield.

Spectrophotometric analysis of purified PtrA eluted off the nickel column revealed an A_{280}/A_{260} ratio much lower than 1. The existence of DNA in purified samples was confirmed by DNA staining when run on a native gel (Figure 3-10). The protein failed to migrate into the native gel as a duplicate gel was run in parallel and stained for protein. DNAse treatment of purified protein did not improve solubility. Purification using a heparin affinity column was also performed but no improvement in

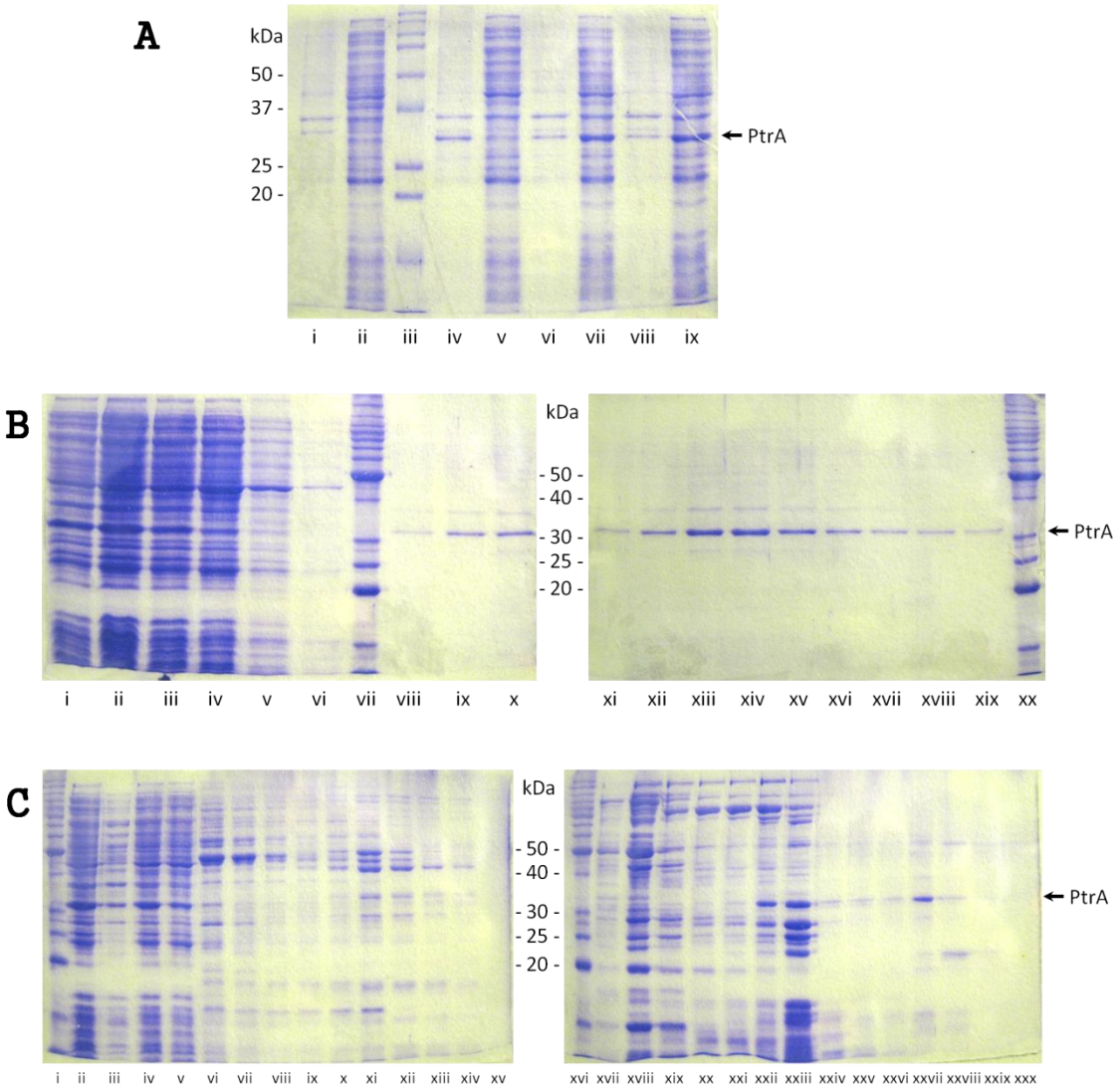

Figure 3-1. SDS-PAGE analysis of His-tagged PtrA overexpression and purification using immobilized nickel-ion affinity chromatography or heparin affinity chromatography. (**A**) Soluble (ii, v, vii, ix) and insoluble (i, iv, vi, viii) fractions of IPTG-induced Rosetta cells transformed with pET28-ptrAFL grown at different induction temperatures. (i, ii) un-induced Rosetta control; (iii) protein size marker; (iv, v) induction at 37°C; (vi, vii) induction at 28°C; (viii, iv) induction at room temperature. (**B**) Purification of His-tagged PtrA from crude extract using a 1 mL HiTrap Chelating HP column in a 50 mM Tris, 0.5 M NaCl, 10% glycerol, and 10 mM imidazole (pH 8) binding buffer: (i) column load; (ii) flow-through; (iii-vi) column wash; (vii) protein size marker; (viii-x) 250 mM imidazole elution step; (xi-xix) 500 mM imidazole elution step; (xx) protein size marker. (**C**) Purification of His-tagged PtrA from crude extract treated with DNase using a 1 mL HiTrap Heparin HP column in a 50 mM Tris, 0.15 M NaCl, 0.1 mM EDTA, and 10% glycerol (pH 8) binding buffer: (i, xvi) protein size marker; (ii) column load; (iii, iv) flow-through; (v-ix) column wash; (x-xv) 250 mM NaCl; (xvii-xxi) 500 mM NaCl; (xxii-xxvi) 1 M NaCl; (xxvii-xxx) 2 M NaCl.

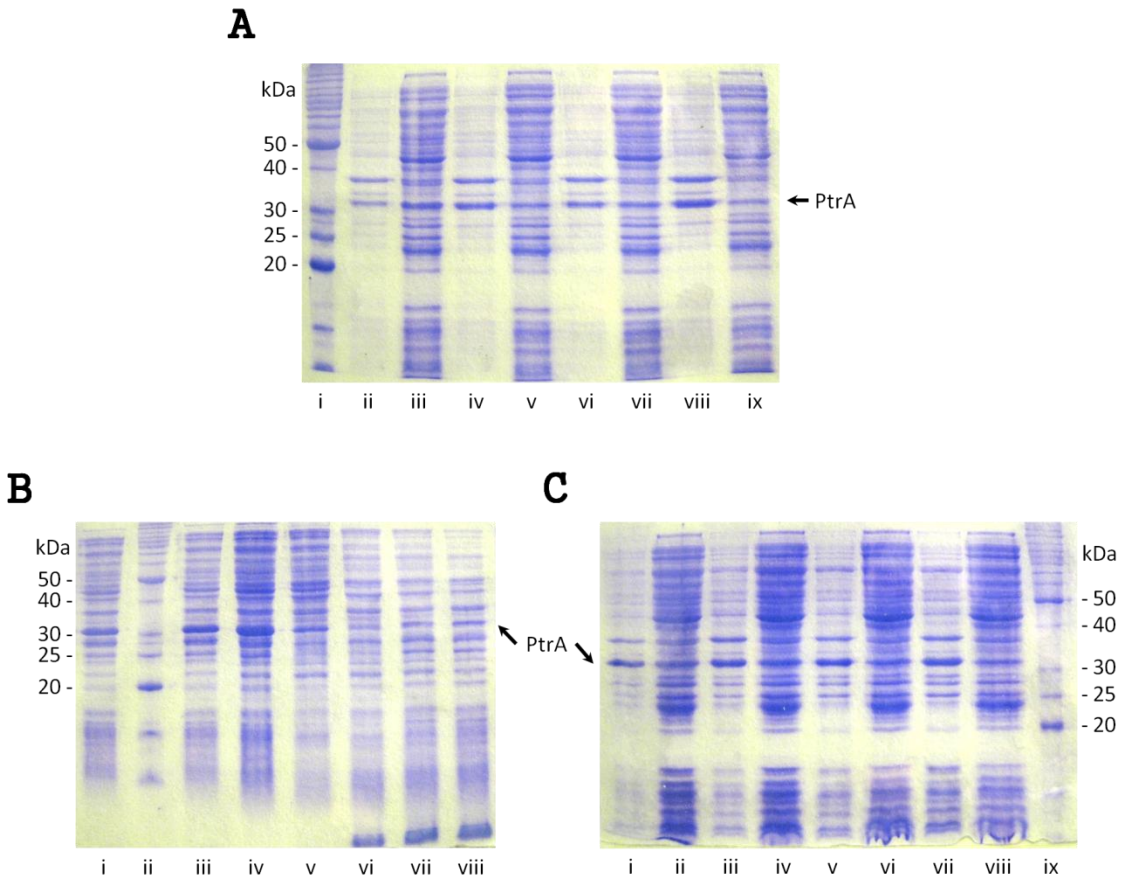

Figure 3-2. SDS-PAGE analysis of the effect of DNAse and nucleic acid precipitants on PtrA. (**A**) Crude extract treated with DNAse and incubated for 30 minutes at 28°C. Insoluble fractions are even-numbered and soluble fractions are odd-numbered: (i) protein size marker; (ii, iii) untreated control; (iv, v) addition of 50 µg/mL DNAse only; (vi, vii) addition of 10 mg/mL $MgCl_2$ only; (viii, iv) addition of both 50 µg/mL DNAse and 10 mg/mL $MgCl_2$. (**B**) Crude extract treated with PEI: (i) untreated crude extract; (ii) protein size marker; (iii) 0% PEI; (iv) 0.05% PEI; (v) 0.10% PEI; (vi) 0.15% PEI; (vii) 0.20% PEI; (viii) 0.25% PEI. (**C**) Crude extract treated with streptomycin sulfate. Insoluble fractions are odd-numbered and soluble fractions are even-numbered: (i, ii) 0.5% streptomycin sulfate; (iii, iv) 1.0% streptomycin sulfate; (v, vi) 1.5% streptomycin sulfate; (vii, viii) 2.0% streptomycin sulfate; (ix) protein size marker.

yield or purity was observed when crude extract treated with DNAse was purified (Figure 3-1). It was then determined that PtrA co-precipitated with nucleic acids when the crude extract was treated with streptomycin sulfate or polyethyleneimine (Figure 3-2). The association of DNA-binding proteins to DNA during protein purification can be exploited, which was the rationale for the next strategy attempted for purifying PtrA.

3. 1. 3. Expression and purification of tagless PtrA

Employing the same PCR primers and restriction enzymes used to construct the His-tagged version of PtrA, the restriction digested PCR product was ligated into a modified, tagless version of pET28b. This second protein construct lacking a purification tag was made to rule out any unintended interactions that may be caused by the His-tag.

3. 1. 3. 1. Recovery and purification of PtrA from nucleic acids

The purification strategy of using nucleic acid precipitants for the purification of DNA-binding proteins closely followed the protocol published by Burgess (1991). Samples containing either streptomycin sulfate or PEI were used to precipitate nucleic acids. To separate PtrA from nucleic acids, a salt gradient was tested to determine the optimal NaCl concentration required to dissociate PtrA from the nucleic acids. The streptomycin sulfate treated sample provided a more pure PtrA sample (Figure 3-3). PtrA eluted from nucleic acids precipitated with streptomycin sulfate was therefore used for further downstream purification using nickel and heparin columns. However, the extra step of isolating PtrA from precipitated nucleic acids did not result in any improvement in yield or purity.

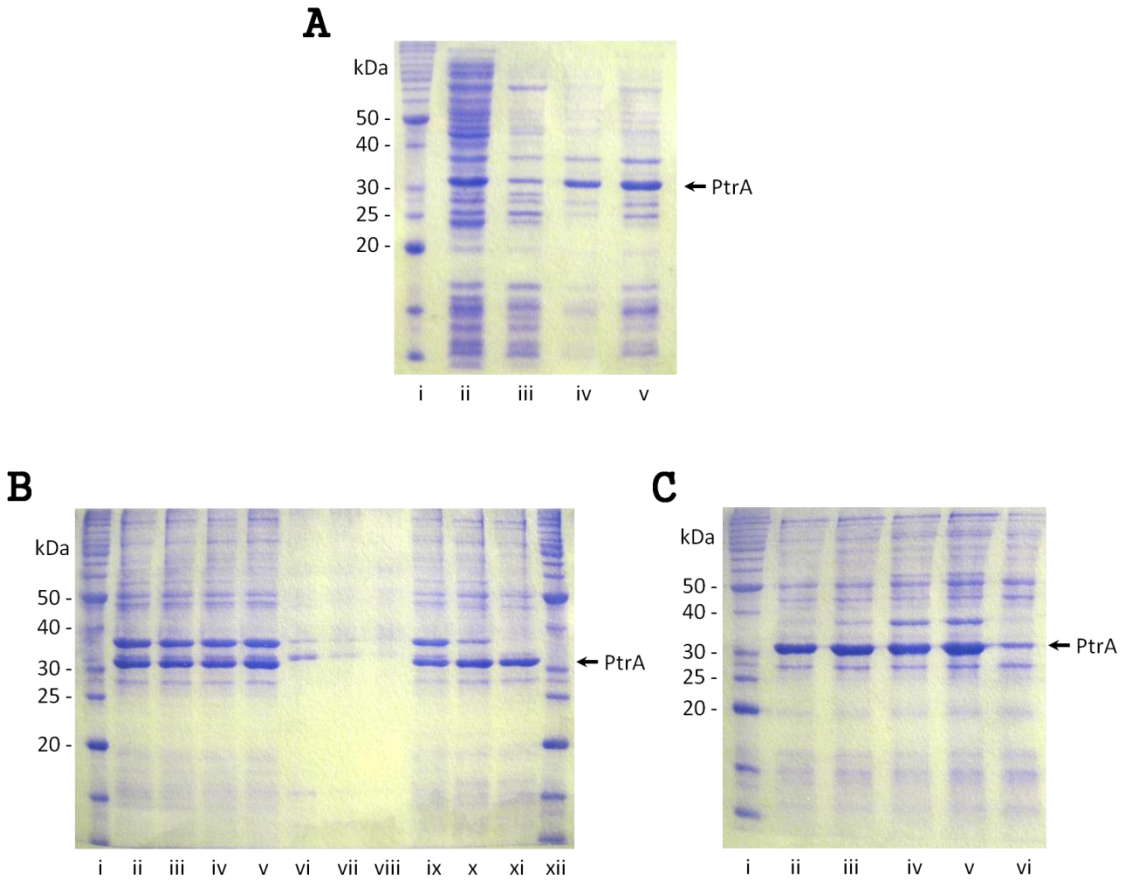

Figure 3-3. SDS-PAGE analysis of PtrA isolated from precipitated nucleic acids and inclusion bodies. (**A**) Partial purification of PtrA isolated from 2.5% streptomycin sulfate precipitated nucleic acids: (i) protein size marker; (ii) crude extract; (iii) supernatant of streptomycin sulfate pellet wash; (iv) supernatant of 0.5 M NaCl elution step; (v) protein sample after 60% ammonium sulfate precipitation and dialysis. Protein shown in *lane v* was used for chromatography purification. (**B**) PtrA inclusion bodies washed with a variety of denaturing reagents: (i, xii) protein size marker; (ii) 0 M urea; (iii) 1 M urea; (iv) 2 M urea; (v) 4 M urea; (vi) 0.2% sarkosyl; (vii) 0.5% sarkosyl; (viii) 1.0% sarkosyl; (ix) 1.0% Tween-20; (x) 1.0% CHAPS; (xi) 1.0% dodecyl maltoside. The dodecyl maltoside wash removed most of the contaminating proteins and was therefore used for further downstream purification steps. (**C**) Solubilisation of PtrA inclusion bodies, washed with dodecyl maltoside, in urea: (i) protein size marker; (ii) 1.0% dodecyl maltoside washed pellet resuspended in 8 M urea; (iii) 0.5% dodecyl maltoside washed pellet resuspended in 8 M urea; (iv) 0.2% dodecyl maltoside washed pellet resuspended in 8 M urea; (v) 0.1% dodecyl maltoside washed pellet resuspended in 8 M urea; (vi) 1.0% dodecyl maltoside washed pellet resuspended in 6 M urea. Denatured protein shown in *lane ii* was used for refolding.

3. 1. 4. Denaturation and refolding of PtrA

Cell cultures were grown in TB and PtrA expression was induced at 37°C. Cells were passed multiple times through the French pressure cell. Following cell lysis and centrifugation, washing of the pellet to remove contaminating proteins and cell debris was performed to improve the downstream refolding process (Maachupalli-Reddy et al., 1997). The pellet was first washed with 1% Triton X-100. A number of different solubilisation agents (urea, sarkosyl, Tween-20, CHAPS, and dodecyl maltoside) were then tested in the next wash step to remove contaminants while retaining PtrA in its insoluble state (Figure 3-3). A second wash step using 1% dodecyl maltoside was judged by SDS-PAGE to be the best washing agent. Thus, all large-scale preparations involving the refolding of denatured PtrA involved a second wash step using dodecyl maltoside.

Reviewed by Singh and Panda (2005), a completely unfolded protein is more prone to aggregation than a partially folded protein intermediate. Therefore, a mild solubilisation procedure as opposed to complete denaturation for refolding proteins was thought to be more successful. Urea and guanidine hydrochloride, chaotropic reagents commonly used for solubilising protein aggregates, were tested for solubilising PtrA. A high concentration of urea, however, was required for complete solubilisation of PtrA (Figure 3-3). An 8 M concentration of urea or 6 M concentration of guanidine hydrochloride was used to solubilise PtrA. Protein refolding by removing denaturing reagents through dialysis as well as on-column was attempted.

3. 1. 4. 1. Refolding of tagless PtrA by dialysis

Initially, refolding of denatured PtrA was attempted by dialysis. Several buffer exchanges were used to remove the denaturants. A step-wise gradient to slowly dialyze out the denaturing reagent, as well as dialysis buffer containing no denaturing reagent for more rapid removal of denaturants were attempted. However, none of the dialysis conditions tested resulted in soluble, refolded protein as visible protein precipitation settled to the bottom of the dialysis tubing. Typically, dialysis buffers contained 20 mM Tris, pH 7.5, and 500 mM NaCl. No buffer additives other than EDTA, βME, and glycerol were attempted in this study.

3. 1. 4. 2. Refolding of His-tagged PtrA on-column

Solubilised, His-tagged PtrA was loaded onto a nickel column for on-column refolding. A decreasing gradient of denaturant concentration in binding buffer was attempted. Surprisingly, no denatured His-tagged PtrA bound to the nickel column; instead, the protein ended up in the flow-through. At this point, efforts were redirected towards working with a truncated version of PtrA.

3. 2. Purification of PtrA-EBD

The insolubility problems of full-length LTTRs are somehow associated with the DBD. Removal of the N-terminal DBD circumvents the problem and allows for the successful purification and structural analysis of truncated LTTR proteins. In this study, a truncated version of PtrA was cloned by removing the DNA sequence corresponding to the first 80 amino acid residues and incorporating an alanine to methionine mutation at

residue 81. The resulting gene encoding the EBD was cloned into the same His-tag vector used for the overexpression of full-length PtrA. Removal of the PtrA-DBD increased protein solubility and maximized binding of PtrA-EBD to the nickel column compared to full-length PtrA (Figure 3-4). A two-step purification protocol consisting of ammonium sulfate protein fractionation and immobilized nickel-ion affinity chromatography yielded a highly pure PtrA-EBD protein sample as judged by SDS-PAGE. A purified PtrA-EBD yield of ~20 mg was obtained per litre of cell culture.

A minimal protein buffer concentration is generally preferred for initial crystallization screening trials to allow for changes in pH when mixed with crystallization solutions. Removal of imidazole from the chromatography elution buffer in preparation for crystallization screens was therefore attempted, but dialyzing out imidazole from the chromatography buffer proved difficult. Initially, a glycine buffer (pH 9.0) supplemented with 10% glycerol was selected after screening a panel of different buffers ranging from pH 4.5-10.5. Buffer exchange from the elution chromatography buffer (50 mM Tris pH 8, 500 mM NaCl, 1 mM TCEP, 350 mM imidazole) into a glycine buffer (50 mM glycine pH 9, 10% glycerol) lacking NaCl or reducing agents resulted in no visible protein precipitation during dialysis. DLS analysis of the protein sample however did reveal protein aggregates. At the time, it was interpreted as a bad sign and glycine was no longer considered as a buffering component. It was also not known that cold temperatures negatively affect the solubility of the protein. Finding an optimal buffer for PtrA-EBD was a challenge.

The effect of buffer additives such as divalent metal cations, glycerol, and reducing agents on protein solubility was analyzed by DLS, leading to the identification

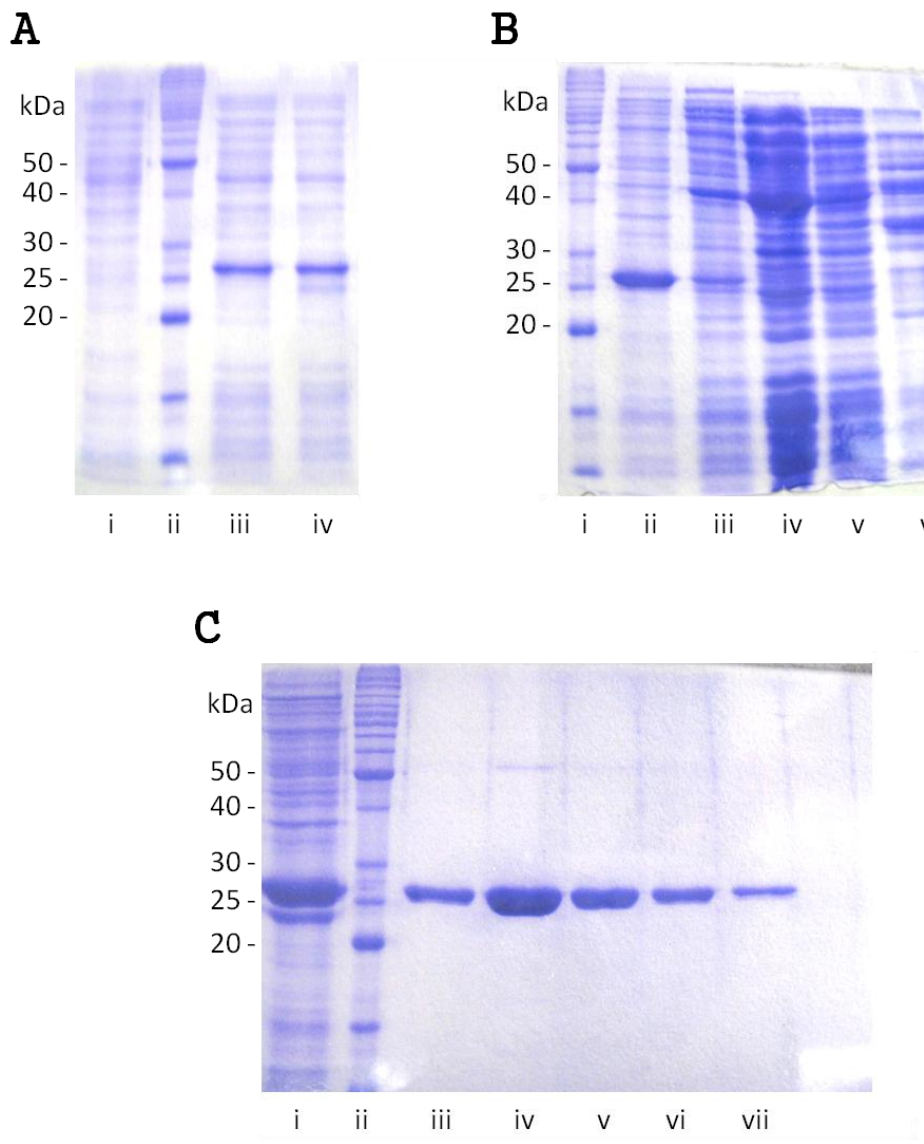

Figure 3-4. SDS-PAGE analysis of protein overexpression and purification of PtrA-EBD using ammonium sulfate fractionation followed by immobilized nickel-ion affinity chromatography. (**A**) Whole cell lysates of PtrA-EBD overexpression: (i) un-induced BL21; (ii) protein size marker; (iii) induced BL21 cells harbouring pET28-ptrAEBD; (iv) induced Rosetta cells harbouring pET28-ptrAEBD. (**B**) Protein from BL21 cells harbouring pET28-ptrAEBD were fractionated by increasing saturations of ammonium sulfate: (i) protein size marker; (ii-vi) resolubilized protein from 30%, 40%, 50%, 60%, and 70% ammonium sulfate fractionated pellets, respectively. (**C**) Purification of PtrA-EBD using Ni-NTA resin: (i) resolubilized and dialyzed protein obtained from 30% ammonium sulfate fraction loaded onto column; (ii) protein size marker; (iii-viii) protein fractions eluted with 350 mM imidazole.

of the reducing agent as a key component required to reduce protein aggregation (Figure 3-5). Interestingly however, while dialyzing against a Tris buffer (pH 8) supplemented with reducing agents and 0.5 M NaCl, the protein sample in the dialysis tubing would first turn cloudy and then eventually revert back to a clear solution. The dialyzed protein was monodisperse when analyzed by DLS and stable at room temperature for longer periods when stored in TCEP as opposed to βME or DTT. The protein was concentrated to ~25 mg/mL and remained monodisperse even after freezing for long-term storage.

Similar to other DNA-binding proteins and successfully crystallized LTTR proteins, PtrA-EBD required a high salt concentration to prevent protein aggregation as determined by DLS analysis. The purified protein buffer for dialysis was optimized to contain 10 mM Tris pH 8, 500 mM NaCl, and 0.5 mM TCEP (Figure 3-5). In this buffer, the protein was concentrated to ~25 mg/mL.

3. 2. 1. Determination of oligomerization state of PtrA-EBD by analytical size-exclusion chromatography and mass spectrometry analysis

The oligomerization state of PtrA-EBD was determined to be a dimer using a Superdex^{TM} 75 column run at room temperature (Figure 3-6). Protein eluted in the first peak, with a calculated molecular weight of 58 kDa, roughly corresponding to twice the molecular weight of a 26 kDa monomer. The oligomerization of PtrA-EBD is in agreement with other LTTR EBD dimers reported in the literature. Solved EBD structures deposited in the PDB show that the dimers take on a more extended conformation rather than globular, which would explain the larger estimated molecular

A

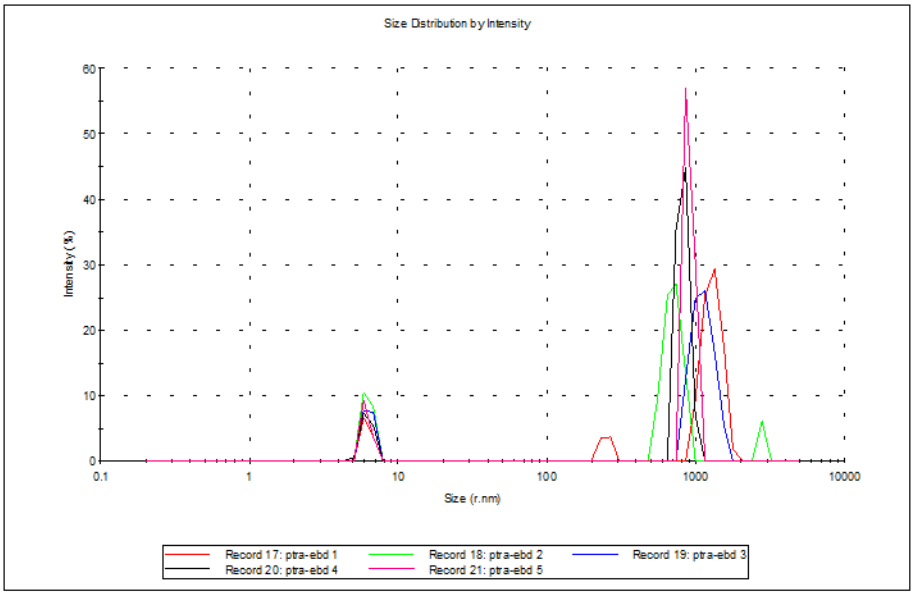

B

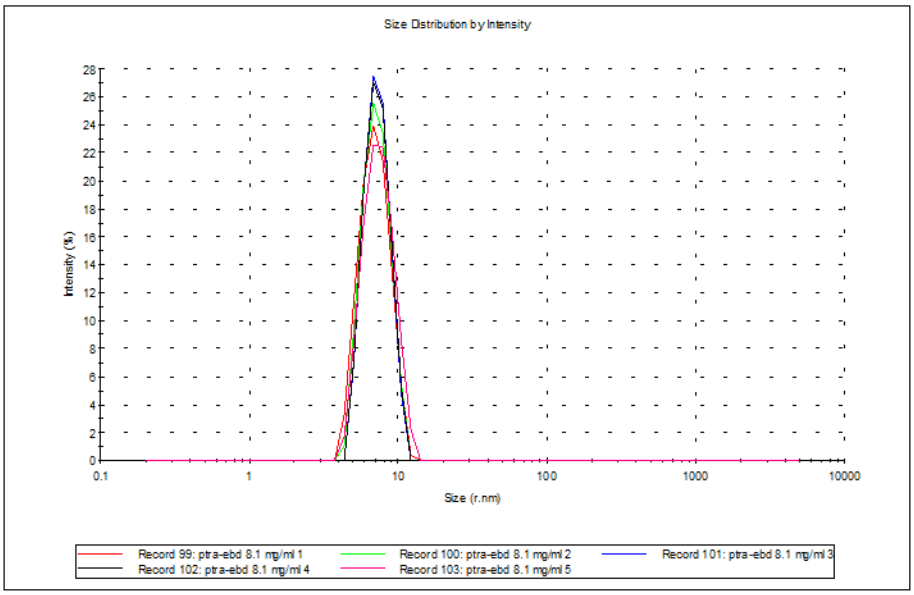

Figure 3-5. Dynamic light scattering analysis of the effect of reducing agents on purified PtrA-EBD monodispersity. (**A**) Analysis of purified PtrA-EBD without reducing agents in buffer. The sample is polydisperse and forms large aggregates as indicated by the multiple peaks. (**B**) Analysis of purified PtrA-EBD in 10 mM Tris, 500 mM NaCl, 0.5 mM TCEP (pH 8). The sample is monodisperse and stable over the duration of DLS analysis.

weight when analyzed by gel filtration chromatography. However, a shoulder observed in the elution peak revealed a non-homogenous population of PtrA-EBD.

Denaturing MS analysis ruled out the possibility of proteolytic cleavage or degradation of the protein sample. The spectrum showed only one major species of a mass of 26117 ± 5 Da, which is in close agreement with 26499 Da calculated using ProtParam tool from the ExPASy online server (Gasteiger et al., 2003; Gasteiger et al., 2005). Non-denaturing MS analysis of purified PtrA-EBD showed the presence of both monomers and dimers (Figure 3-6). The dimers, however, are non-covalently associated together as denaturing MS analysis showed only one ion envelope corresponding to the monomer. The two sub-populations of monomers and dimers could not be distinguished by DLS analysis.

Buffer exchange was necessary for MS analysis, but it was likely that dialyzing the protein against a non-optimized buffer caused the protein to aggregate. Denaturing MS analysis of a protein sample prepared in the cold showed the presence of both monomers and dimers. Precipitated protein, washed off the dialysis membrane using a 1% acetic acid and 50% methanol solution, failed to dissociate into only monomers. MS analysis of the aggregated protein suggested that there is some sort of covalent modification between monomers. The spectrum showed evidence of protein aggregates of higher order than a dimer that was more pronounced when the protein was dialyzed at 4°C instead of room temperature. A temperature effect was also obvious when a 30-µL aliquot of purified protein was concentrated to 25 mg/mL. When placed on ice, the solution turned cloudy-white in appearance. When taken off ice, the solution reverted to a clear solution.

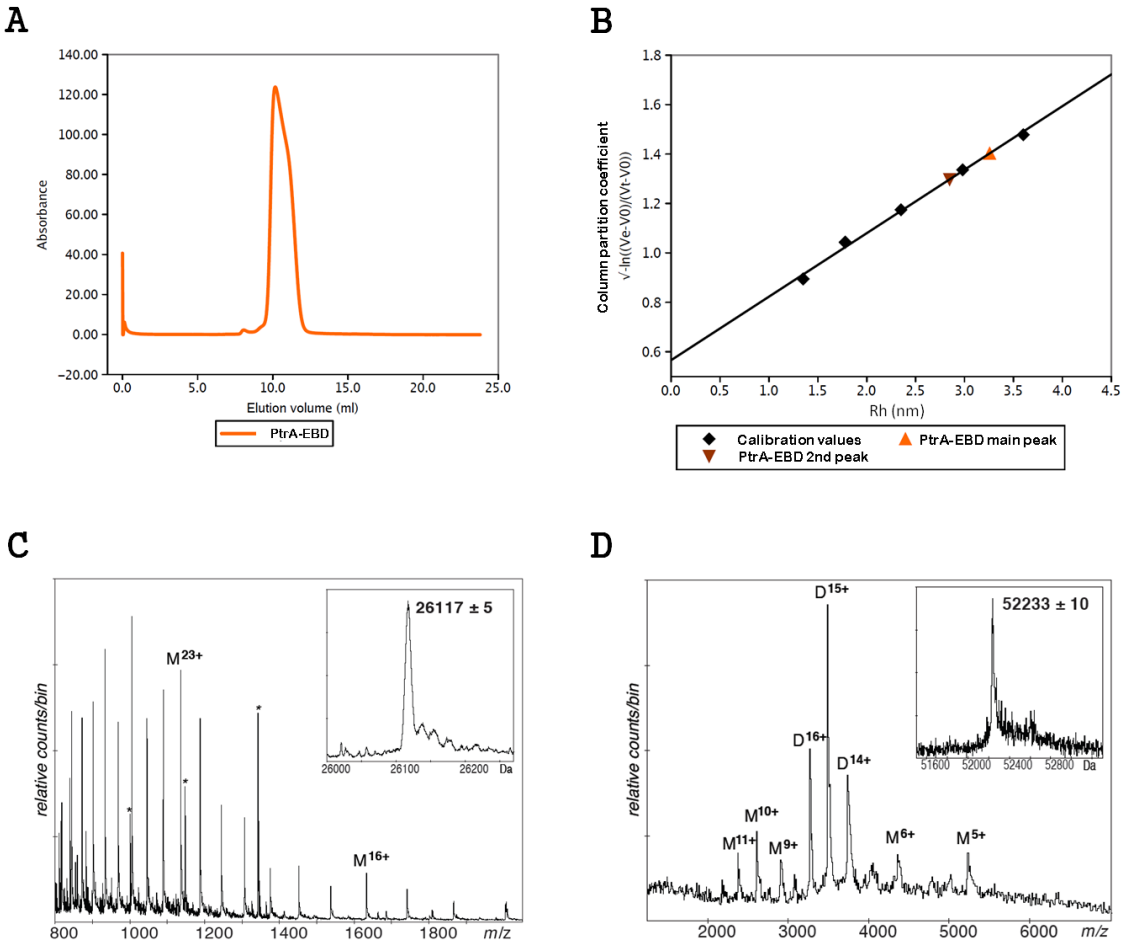

Figure 3-6. Gel filtration and MS analysis of purified PtrA-EBD. (**A**) FPLC trace of purified PtrA-EBD run on a gel filtration column at room temperature. (**B**) Calibration curve of the gel filtration column using known protein size standards: aprotinin (6.5 kDa); cytochrome c (12.4 kDa); carbonic anhydrase (29 kDa); ovalbumin (43 kDa); conalbumin (75 kDa). Estimated based on the elution time of PtrA-EBD, the main and shoulder peaks correspond to a calculated molecular weight of 58 kDa and 42 kDa, respectively. (**C**) Part of the ESI spectrum of denatured PtrA-EBD showing one major ion envelope of a species with a calculated mass of 26117 ± 5 Da shown in the inset. The ions marked with * are singly charged and are of unknown origin. (**D**) Part of the nanospray ionization spectrum of non-denatured PtrA-EBD showing two ion envelopes corresponding to that of a monomer (5+ to 11+) and dimer (13+ to 17+). The calculated mass of the dimer is 52233 ± 10 Da shown in the inset.
N.B. Gel filtration run and generation of graphs for Panels A and B were performed by Dr. Markus Meier, Department of Chemistry, University of Manitoba. MS experiments and generation of graphs for Panels C and D were performed by Dr. Lynda Donald, Department of Chemistry, University of Manitoba.

The effect of reducing agents, which were necessary to keep PtrA-EBD in solution, was assessed by non-denaturing SDS-PAGE. Non-reduced and reduced PtrA-EBD protein samples were run on a SDS-PAGE gel (Figure 3-7). A double-band of protein was observed in non-reducing conditions. The double-band disappeared when reducing agents were added, which suggested that an internal redox modification was formed within a subpopulation of PtrA-EBD monomers. This modification may be the initial step of protein aggregation, resulting in a misfolded protein which is unable to form a dimer in solution.

3. 2. 2. Crystallization of PtrA-EBD

Initial success in obtaining protein crystal was achieved using 96-well plates (Figure 3-8). A complete list of all crystal screens used is shown in Table 3-2. However, optimizing the conditions that yielded crystal growth, by scaling up the crystallization drop volumes in 24-well plates and by varying the pH, salt, and precipitant concentrations, was unsuccessful. Two of the crystallization conditions were not reproducible in the 24-well plate format. Amorphous precipitation was consistently observed in the larger drop volumes contained in the 24-well plates despite lowering protein concentrations; visible protein precipitation was not otherwise observed in the crystallization drops that gave rise to crystal growth in the 96-well plates. Adding 1-5 mM TCEP to the protein sample and crystallization solutions, varying hanging drop volumes or protein concentrations, and degassing the solutions did not improve crystal growth. One crystal growth condition was reproducible in the 24-well plate format, but only the formation of microcrystals was observed (Figure 3-9).

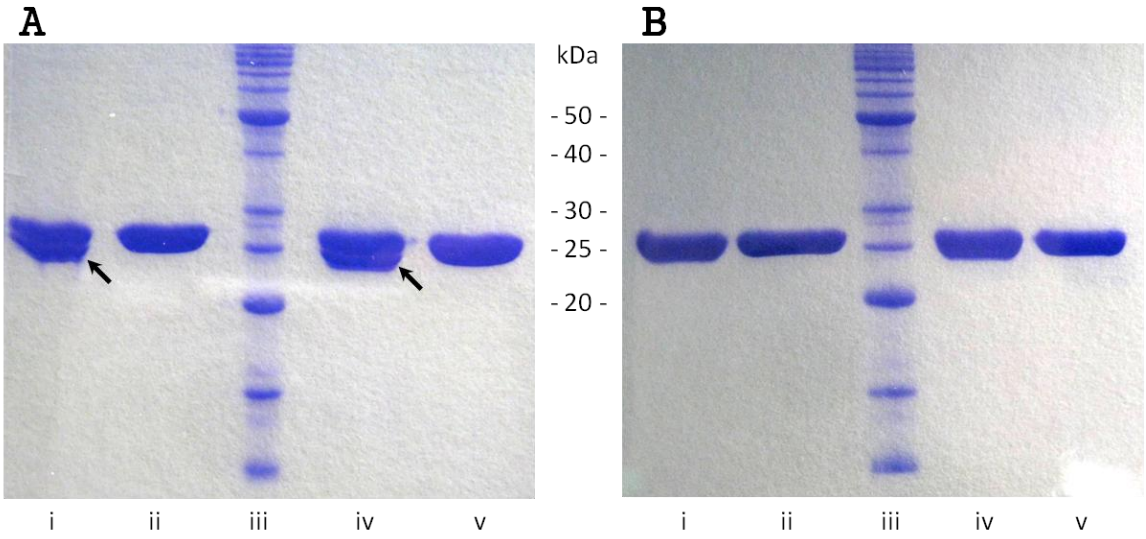

Figure 3-7. Reducing and non-reducing SDS-PAGE analysis of purified PtrA-EBD and refolded PtrA-EBD. (**A**) Freshly purified PtrA-EBD was analyzed by SDS-PAGE in sample buffer with βME (ii, v) and without βME (i, iv). Protein samples in *lanes i* and *ii* were not boiled after the addition of sample buffer; (iii) protein size marker. As indicated by the arrows, a double band was observed in the two lanes containing no reducing agents in the sample buffer. (**B**) Denatured and refolded PtrA-EBD in the the presence of reducing agents analyzed by SDS-PAGE in sample buffer with βME (ii, v) and without βME (i, iv). Protein samples in *lanes i* and *ii* were not boiled after the addition of sample buffer; (iii) protein size marker. No protein double-banding pattern was observed.

Table 3-2. Summary of 96-well crystallization screens performed on PtrA-EBD.

Screen name	Protein concentration (mg/mL)
Classics I	6.6, 8.1[a], 25.2
Classics II	1.4, 2.9, 5.7, 6.6[b], 8.1, 25.2
PEGs	5.0, 6.6, 10.0, 15.0, 25.2
PEGs II	5.0, 6.6, 10.0[c], 25.2
$AmSO_4$	5.5, 10.9, 24.2

[a] produced crystals in 0.1 M HEPES sodium salt pH 7.5, 10% (v/v) isopropanol, 20% (w/v) PEG-4000
[b] produced crystals in 1.5 M ammonium sulfate, 0.1 M Bis-Tris pH 6.5, 0.1 M NaCl
[c] produced crystals in 0.1 M tri-sodium citrate, 5% (v/v) isopropanol, 20% (w/v) PEG-4000

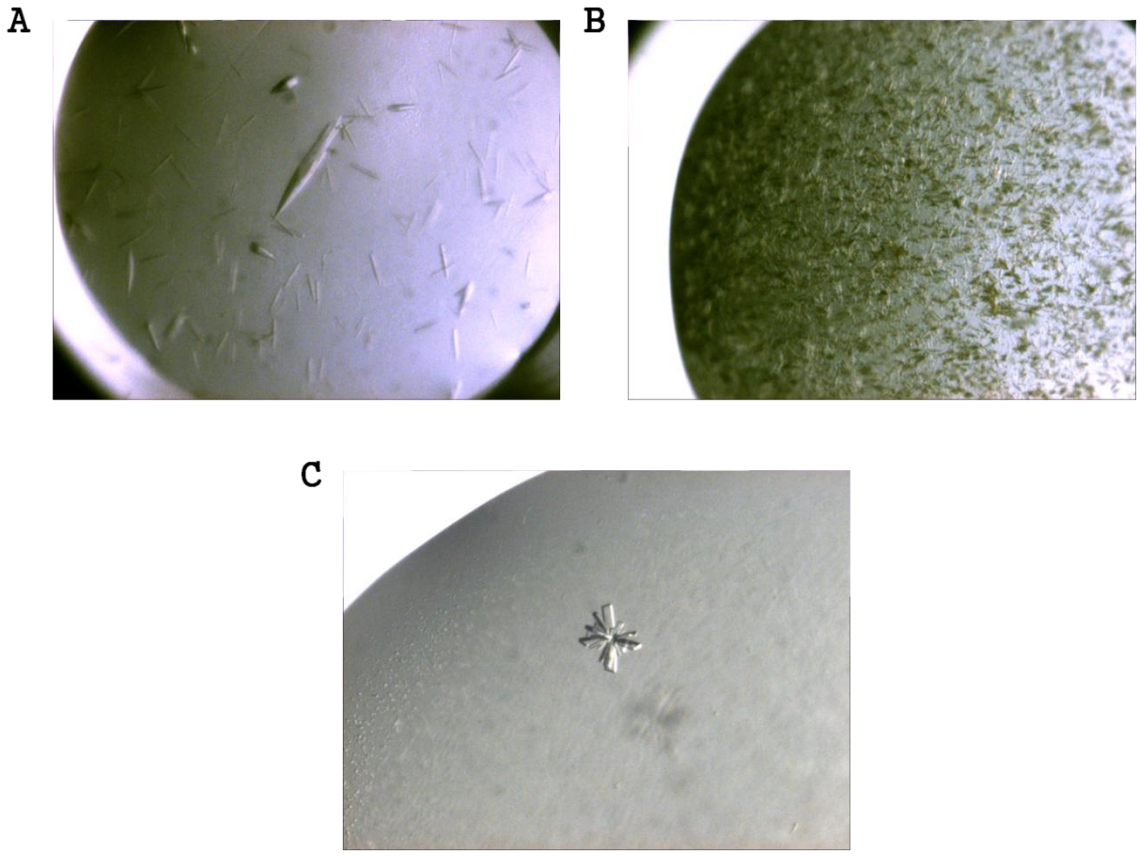

Figure 3-8. Pictures of the different screening conditions that produced crystals in 96-well plates. (**A**) Needle-like crystals formed in Classics I Suite screen containing 0.1 M HEPES sodium salt pH 7.5, 10% (v/v) isopropanol, and 20% (w/v) PEG-4000 mixed with 8.1 mg/mL PtrA-EBD. (**B**) Microcrystals formed in PEGs II Suite screen containing 0.1 M tri-sodium citrate, 5% (v/v) isopropanol, and 20% (w/v) PEG-4000 mixed with 10.0 mg/mL PtrA-EBD. (**C**) Crystal cluster formed in Classics II Suite screen containing 1.5 M ammonium sulfate, 0.1 M Bis-Tris pH 6.5, and 0.1 M NaCl mixed with 6.6 mg/mL PtrA-EBD.

Figure 3-9. Picture of microcrystals grown in a 24-well plate by hanging drop vapour diffusion method. The drop contained 2.9 mg/mL PtrA-EBD in 10 mM Tris pH 8, 500 mM NaCl, 1 mM TCEP diluted with an equal 1-µL volume of mother liquor containing 1.5 M ammonium sulfate, 0.1 M Bis-Tris pH 6.4, 0.1 M NaCl.

It was concluded that the propensity for PtrA-EBD to readily oxidize was hindering crystal growth. Denaturing and refolding of PtrA-EBD in the presence of reducing agents yielded a more reduced population of protein as no double band was observed on the SDS-PAGE gel (Figure 3-7). The PtrA-EBD protein treated with this addition denaturing and refolding step was performed just prior to the writing of this thesis; it was therefore not subjected to crystallization screening trials.

3. 3. Identification of PtrA cognate binding sites within the *ptrA* promoter

Preliminary studies have shown that *ptrA* positively autoregulates its own expression. Positive autoregulators of the LTTR family are far less common than negative autoregulators in the literature. The mechanism of positive autoregulation remains poorly understood compared to negative autoregulation by members of the LTTR family.

3. 3. 1. Electrophoretic mobility shift assays

At the time of study, only purified His-tagged PtrA eluted from a nickel column was used for the EMSAs. Although the concentration of purified PtrA was too low for crystallization trials, it was sufficient for gel shift assays. Freshly purified protein samples were diluted and used immediately for gel shift assays. The DNA:protein molar ratios were calculated based on the molecular weight of the PtrA monomer.

Even though the disappearance of probe DNA band was evident, a clear shift between bound and unbound DNA was not obvious (Figure 3-10). Purified protein

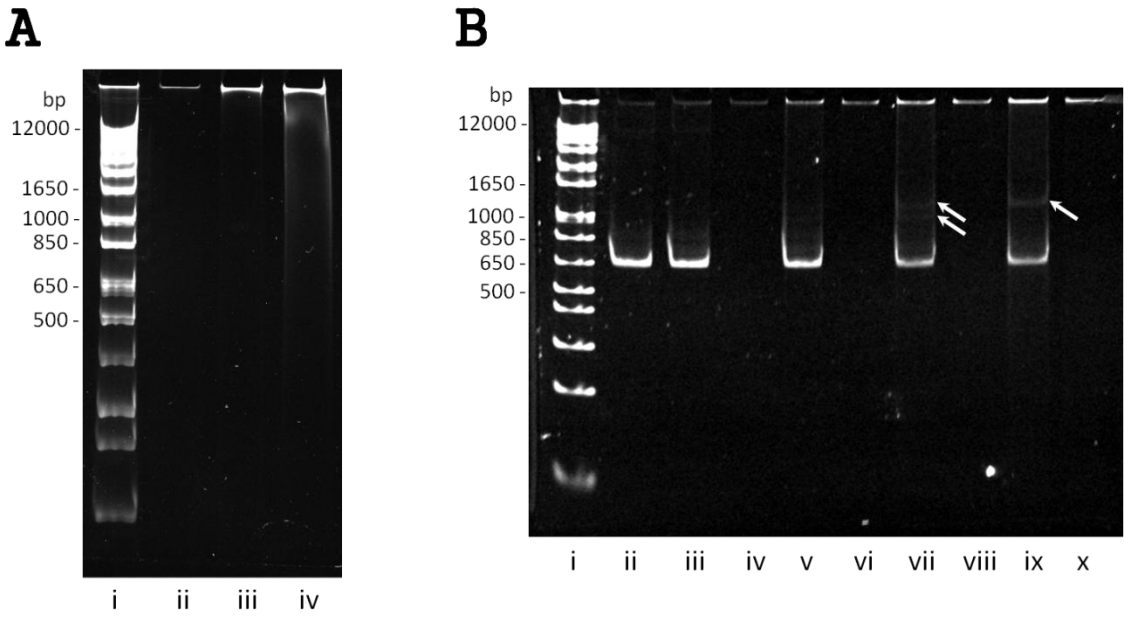

Figure 3-10. Native-PAGE analysis and EMSA of purified PtrA in the presence and absence of *ptrA* promoter DNA. (**A**) DNA co-purified with PtrA as shown by DNA staining. PtrA protein was purified using condition 7^{α} listed in Table 3-1 and run on a 5% polyacrylamide native gel. (i) DNA size marker; (ii) purified PtrA pre-treated with DNAse prior to chromatography purification; (iii) denatured PtrA (by boiling); (iv) non-denatured PtrA. (**B**) EMSA of purified PtrA from crude extract treated with DNAse prior to nickel column purification using condition 7^{α} listed in Table 3-1. A white arrow indicates a visible but faint DNA band. A concentration of 0.5 pM 631-bp DNA probe containing the *ptrA* promoter upstream of the translation start site was run in *lanes ii, iii, v, vii,* and *ix*. *Lanes iv, vi, viii,* and *x*, contained protein but no probe DNA. Concentrations of protein run in each lane were: (iii, iv) 0.125 pM; (v, vi) 0.5 pM; (vii, viii) 1 pM; (ix, x) 3 pM. *Lane i* contains a DNA size marker.

samples failed to migrate into the gel and lanes containing protein in the absence of probe DNA was contaminated with DNA carried over from purification. Adding DNAse to the lysis buffer during purification, incubating DNAse with PtrA bound to the nickel column, and washing the column with a 2 M NaCl concentration failed to remove all traces of DNA from purified PtrA samples. DNAse from the purified protein sample was also not completely removed despite excessive washing of the column with buffer. Residual DNAse activity was evident, even with the addition of EDTA to the EMSA buffer, as indicated by the faint smearing of DNA below the probe DNA band. Because of these issues, an alternative to EMSAs was sought.

3. 3. 2. β-galactosidase assays

Fragments of the *ptrA* promoter upstream of the translational start site were fused to a promoterless *lacZ* in order to assess the transcriptional activity *in vivo*. The promoter fragments cloned into pLP170 are separated from *lacZ* by an RNAse splice site, allowing for the independent translation of the *lacZ* gene product β-galactosidase. A visual depiction of the different *lacZ* transcriptional fusion constructs transformed into PA23 is shown in Figure 3-11. Using round-the-horn PCR site-directed mutagenesis, mutation of the T-N_{11}-A box from a 5′-TTTCAAATGGAAA-3′ sequence to a 5′-CGACAACTGGAAC-3′ sequence resulted in no change in transcriptional activity (Figure 3-11). The other *ptrA* promoter constructs were cloned using non-mutagenic PCR primers. The β-galactosidase results suggest that positive autoregulatory elements lie somewhere between 52-198 bp region upstream of the PtrA translation start site.

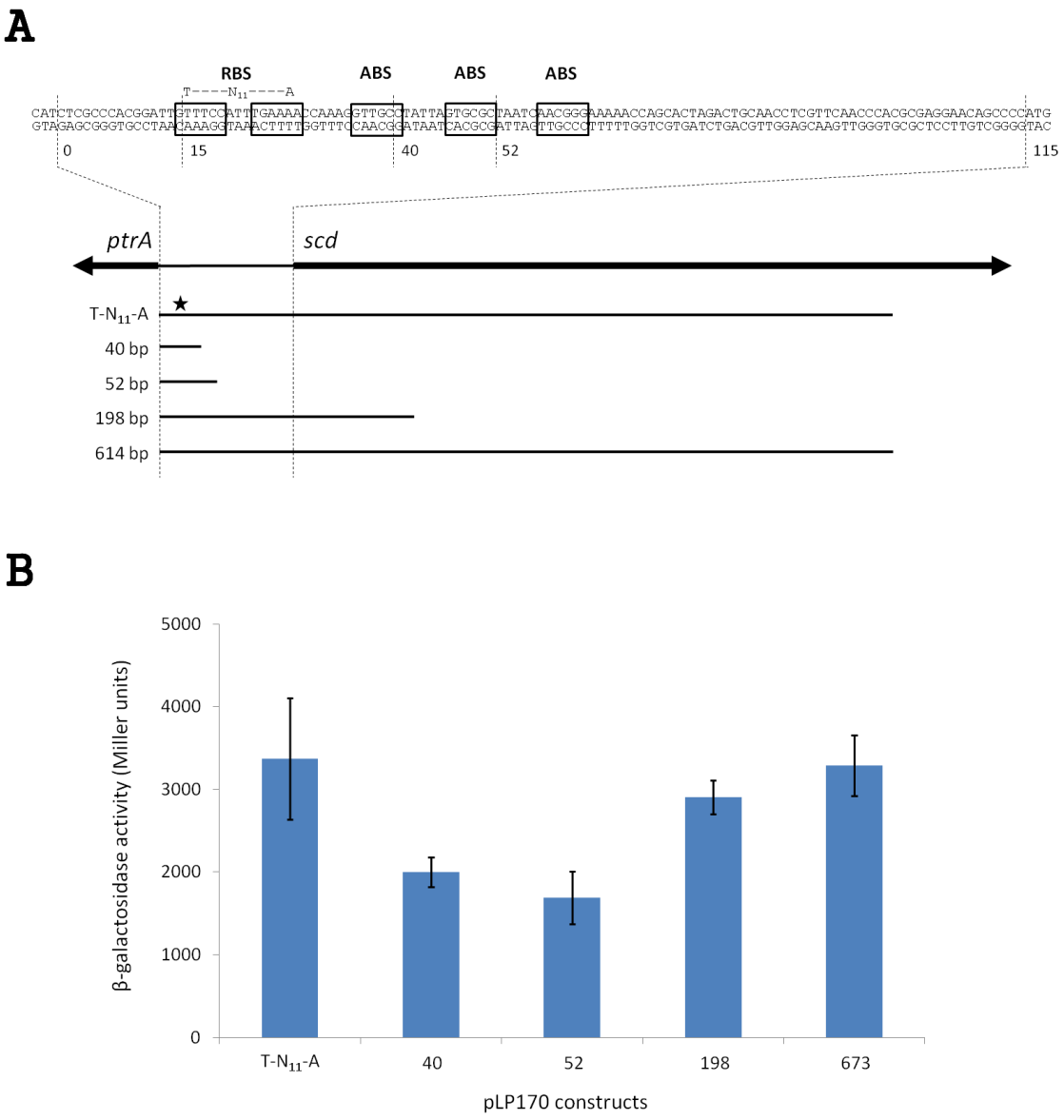

Figure 3-11. Beta-galactosidase activity of *ptrA* promoter truncations in *P. chlororaphis* PA23. (**A**) Diagram of the different *ptrA* promoter fragments cloned into pLP170 and transformed into PA23. The numbering of each fragment refers to the number of bp upstream of the PtrA translational start site; each promoter truncation contains an additional 676 bp downstream of the translational start site. The hypothesized location of the RBS and ABS binding sites are modeled after *atzR* from *Pseudomonas* sp. strain ADP (Porrúa et al., 2010). The location of the mutated T-N_{11}-A binding motif, starting at 15-bp upstream of the PtrA translational start site, is denoted by a star. The intergenic region between the translational start sites of *ptrA* and *scd* (annotated as a short-chain dehydrogenase) is 115 bp. Regulation of the divergent *scd* gene by *ptrA* is not yet known. (**B**) Beta-galactosidase activity of the *ptrA* promoter truncations were monitored after 24 hours of culture growth in PTSB. Activities ± SD measured in Miller units are the mean values of triplicate samples.

4. DISCUSSION

4. 1. Full-length PtrA

Solubility issues are notoriously problematic for LTTRs. PtrA proved to be no exception. Purified protein samples were not stable and readily precipitated after short-term storage at 4°C or room temperature. Attempts to concentrate the protein sample were unsuccessful. Results from purifying the EBD suggest that the protein should be purified at room temperature and in the presence of reducing agents, but this was not known at the time of full-length PtrA purification trials. Furthermore, binding of PtrA to *E. coli* DNA may contribute to the insolubility problems encountered.

As reviewed by Maddocks and Oyston (2008), the insolubility issues are often associated with the DBD. Co-precipitation of PtrA with nucleic acids and DNA contamination with IMAC purified PtrA show that the protein is bound to DNA. The low PtrA yield obtained during purification could be due to the burying of His-tags within the quaternary structure if the protein functions as oligomers of orders higher than dimers, particularly when solved full-length LTTR structures to date show that dimers are arranged in a head-to-tail fashion. The bound DNA may also physically occlude binding of protein to the column, particularly when a high degree of DNA bending can occur upon binding of LTTRs (van Keulen et al., 1998; Akakura and Winans, 2002a, b). Interestingly however, there was no evidence of PtrA binding to a nickel column when the protein was denaturated in 8 M urea or 6 M guanidine hydrochloride. It is possible that the covalent modifications observed during the purification of PtrA-EBD may also be occurring with the full-length protein, which somehow prevents the His-tag from

being exposed. It is not clear why the denatured full-length protein does not bind to a nickel column, but removal of the DBD results in optimal binding of the truncated protein to a nickel column.

Finding a suitable buffer for increasing the solubility of the full-length protein was elusive, despite many attempts. Drop-wise dilution of purified protein into different buffers of varying pH followed by visual inspection for solubility was unsuccessful in all cases. A panel of lysis buffers containing different buffering reagents (MES, Tris, CAPS, sodium phosphate), pHs (6.0 - 10.0), salt concentrations (0.5 - 2.0 M), and other additives (DNAse, EDTA, glycerol, urea, detergents, and reducing agents) were screened for enhanced solubility after cell lysis, but none of the conditions revealed a discernible increase in protein solubility as judged by SDS-PAGE. A more rigorous method for assessing protein solubility after purification such as those suggested by Jancarik et al., (2004) and Howe (2004) should be pursued. The use of crystallization screening solutions can also be considered a robust method for identifying conditions that increase protein solubility (Collins et al., 2005). Drops that remain clear indicate a condition that favors better protein solubility. In the proper buffer, non-specific aggregation can be limited, which may ultimately lead to an increase in protein concentration more amenable to protein crystallization. Resolving the solubility issues is also necessary for EMSAs and other DNA-binding experiments to be successfully performed.

Identifying cognate binding sites and the co-inducer molecule of PtrA may aid in enhancing protein solubility. PtrA was able to bind to a heparin column, but when the protein was eluted, it rapidly precipitated. The addition of DNA oligomers containing a high-affinity DNA recognition sequence may increase the solubility of the protein. The

effect of co-inducer binding to PtrA is not known, but bound ligands can increase the solubility of proteins (Vedadi et al., 2006). Identification of the PtrA co-inducer molecule is an ongoing area of research. Structural characterization of the EBD will aid in identifying the co-inducer molecule.

Preliminary results of denaturing and refolding the EBD with reducing agents suggest that a similar strategy could also be successful for the full-length protein. The helix-turn-helix motif has been reported in the literature to fold quickly and independently as a domain (Religa et al., 2007). Although the winged extension of the helix-turn-helix motif and the flexible linker region joining the DBD to the EBD may complicate the refolding process, refolding of full-length PtrA was by no means exhaustively attempted in this study. Varying pH, refolding at temperatures other than 4°C, and adding refolding chaperones and other additives known to help in the refolding process (Tsumoto et al., 2003; Alibolandi and Mirzahoseini, 2011) were not tried. More importantly, the addition of reducing agents should be included throughout the denaturing and refolding process as it was required for the purification of PtrA-EBD. Drop-wise dilution method for refolding proteins is also a robust method for successful protein refolding and should be attempted as well (Clark, 1998; Tsumoto et al., 2003; Dechavanne et al., 2011).

Other possible purification strategies to pursue may be creating an N-terminal His-tagged protein or changing the expression system. As reported in the literature, a full-length LTTR His-tagged on the N-terminus was successfully purified and crystallized (Law et al., 2009). In this study, a cell-free expression system was never attempted. Although labour-intensive, a cell-free system would eliminate any non-

specific binding of PtrA to *E. coli* DNA and potentially other LTTRs. Other affinity tags to purify the full-length protein also warrant future consideration, such as a longer linker region adjoining the His-tag, glutathione S-transferase tag, or a maltose-binding protein fusion, which are known to help increase the solubility of proteins.

4. 2. PtrA effector binding domain

A two-step purification of the EBD yielded a highly pure protein sample, but it is not clear what is occurring to the protein during dialysis, and why reducing agents can reverse protein aggregation. High concentrations of reducing agents were required for the purification of solved full-length structures of DntR (Smirnova et al., 2004), TsaR (Monferrer et al., 2008), and BenM (Ruangprasert et al., 2010). Degassing the buffers made no observable difference on reducing protein aggregation during dialysis. There are two cysteines in the amino acid sequence of the EBD, and structure prediction software using SWISS-MODEL (Arnold et al., 2006; Kiefer et al., 2009; Peitsch, 1995) suggest that the cysteines are exposed on the surface of the protein. Free reactive cysteines could be one possible explanation for the aggregation problems encountered. Mutating the cysteines is a possible avenue to explore.

Selecting a different buffer may increase the solubility of the protein. For example, the aforementioned glycine buffer without added reducing agents and NaCl resulted in no visible protein precipitation during dialysis. Glycine is commonly used as a protein stabilizer and as an additive for protein refolding, and was successfully used to refold a *lysA* mutant (Bourot et al., 2000). Biophysical analysis of PtrA-EBD buffered with glycine and other additives should be performed. Glycerol has also been

demonstrated to reduce the amount of reducing agent required for purifying and storing LTTR proteins (Monferrer et al., 2008; Ruangprasert et al., 2010). Trace transition metals, such as nickel ions leached from the column, can catalyze oxidative reactions (Aust et al., 1985). The effect of adding glycerol and EDTA should be analyzed. In the case of PtrA-EBD, DLS analysis is only sufficient to detect large aggregates and could not distinguish monomers from dimers. Analytical gel filtration chromatography will be required for detecting non-homogeneity of PtrA-EBD samples.

Difficulty in obtaining crystals and optimizing crystal growth conditions may be explained by the monomer-dimer equilibrium. Formation of crystals was observed in three of the conditions screened, but attempts to optimize crystal growth when scaling up the drop sizes proved to be ineffective and irreproducible for two of the conditions. Difficulty in reproducing crystal hits may have been exacerbated by interchanging between sitting-drop and hanging-drop vapour diffusion methods. Initially, crystal screening conditions were performed in the 24-well plates using Hampton Classics Screen™ containing 48 different solutions but no crystal growth was observed. Screening for crystallization conditions should not have been abandoned so early in the 24-well plates and further attempts should be considered; crystallization screens and optimization of crystal growth conditions should have been performed in the same plate format. Other crystallization methods such as seeding and microbatch under oil may yield better quality crystals. The microbatch crystallization method was necessary for solving the full-length BenM structure (Ruangprasert et al., 2010). Different seeding techniques can also improve crystal growth and yield larger crystals (Bergfors, 2003).

Neither of these methods was attempted over the course of this study, but warrant future consideration.

Perhaps the most promising and logical route for obtaining diffraction-quality crystals to solve the EBD structure is to optimize crystal growth conditions in the 96-well plates rather than 24-well plates. As reviewed by Chayen and Saridakis (2008), laboratories have successfully optimized crystal growth conditions with drop sizes of 200 µL to produce quality crystals for x-ray diffraction. In the case of this study, the conditions that produced protein crystals in the 96-well plates were devoid of visible protein precipitation in the crystallization drops. When scaling up the drop sizes into the 24-well plates, substantial amorphous precipitation was observed even when varying hanging drop volumes and decreasing protein concentrations. Preliminary crystallization conditions have already been discovered in the 96-well plates, therefore optimizing crystal growth conditions in the same plate format should be performed in future studies.

Denaturing and refolding of PtrA-EBD was also performed to successfully eliminate the double-banding pattern of PtrA-EBD when run on a non-reducing SDS-PAGE gel. It is believed that an internal covalent modification is occurring within a PtrA-EBD monomer, resulting in a smaller apparent molecular weight species when run on a denaturing SDS-PAGE gel. The nature of the covalent modification is not known, but the double-band disappears when reducing agent is added to the sample buffer. It is hypothesized that the reduced and non-reduced form of PtrA-EBD is the reason for the shoulder in the elution peak when analyzed by gel filtration. As a result, the monomer-dimer equilibrium may be impeding the growth of quality crystals. However, biophysical

analysis of the refolded protein was not performed whether or not the protein is properly folded had not been determined at the time of writing.

4. 3. Autoregulation of *ptrA*

Attempts to bind PtrA to DNA binding sites and visualize gel shifts of the DNA were unsuccessful presumably because of solubility issues related to PtrA. Purified protein alone run on a native PAGE gel failed to migrate into the gel as stained protein outlined the bottom of the wells. Encouragingly, faint evidence of a shift in DNA band was observed as shown in Figure 3-10. As discussed previously, finding an optimal buffer condition that increases the solubility of PtrA may prevent protein aggregation and allow for the migration of protein into the gel. Increasing the solubility of the protein in solution may also allow for other DNA-binding assays to be performed, such as DNAse footprinting. The contamination of purified PtrA with DNA may be an issue that needs to be resolved as well. A combination of DNAse treatment and a high concentration of salt run through the column failed to remove all traces of DNA. The method for recovering PtrA from streptomycin sulfate precipitated nucleic acids could provide an additional method for removing DNA without denaturing the protein.

For this study, β-galactosidase assays were performed as an alternative to elucidate the cognate binding sites of *ptrA*. The strategy for truncating the *ptrA* promoter region was modelled after the well-characterized AtzR LTTR (Porrúa et al., 2010). It was hypothesized that the removal of essential binding regions of PtrA would result in a change in transcriptional activity measured in Miller Units. The results shown in Figure 3-11 suggest that PtrA may bind to a region between 52 and 198 bp upstream of the

translational start site. Promoter truncations within this region need to be created in order to identify the location and sequence of potential binding sites. At the time of study, a *ptrA* mutant compatible with β-galactosidase assays was not yet created. Ongoing efforts in creating a *ptrA* mutant strain are essential for understanding the autoregulatory role of *ptrA*. Different culture time points should also be performed once the binding sites have been identified. Culture density affects the transcription of *ptrA* but preliminary studies have thus far shown that *ptrA* is maximally expressed during the onset of stationary phase.

It is still not known what genes are regulated by *ptrA*. Currently, work is being done to determine whether or not the divergent *scd* gene is regulated by *ptrA* (N. Klaponski). The intergenic region separating the two genes contains 115 bp. The few positive autoregulators that have been characterized repress the expression of target genes, which are usually other transcriptional regulators (Harris et al., 1998; Guy et al., 2000; Mukherjee et al., 2000; Lehnen et al., 2002; Heroven and Dersch, 2006; Axler-DiPerte et al., 2009). But it is possible for the binding sites of different transcriptional regulators to overlap. For example, the positive autoregulator SpvR counteracts the action of another repressor by competing for the same overlapping binding sites (Marshall et al., 1999). The co-inducer molecules for the positive autoregulators reported in the literature have yet to be identified. Binding sites a few hundred bp upstream and downstream of the transcriptional start site have also been observed for GcvA (Wilson et al., 1995) and LadA (Viswanathan et al., 2007). Assessing the transcriptional regulatory role of *ptrA* on the divergent *scd* gene may provide further insight in identifying *ptrA* binding sites.

4. 4. Conclusions

This study was the first investigation of *ptrA* at the molecular level. The insolubility problems encountered during the purification of full-length PtrA made structural characterization of the protein impossible and hampered EMSAs. When overexpressed in *E. coli*, PtrA was found to be bound to DNA, which appeared to increase the solubility of the protein. Complete removal of DNA from IMAC purified protein proved difficult even with a combination of a high salt wash and DNAse treatment. PtrA purified from a heparin column was unstable and precipitated quickly. Purification of PtrA from precipitated nucleic acids, or denaturing and refolding the protein were unsuccessfully performed in this study for the conditions attempted. Difficulties in increasing yield and purity were further complicated by the low stability of protein in solution.

Removal of the DBD resulted in optimal binding of the protein to the nickel column. With the addition of reducing agents, purified PtrA-EBD stayed in solution when stored at room temperature for weeks. Despite a non-homogenous population of monomers and dimers coexisting in solution, preliminary crystallization of PtrA-EBD was successful.

Gel shift assays were also performed by using IMAC purified PtrA. Although the probe DNA band was disappearing upon incremental addition of protein and a faint shift was observed, the majority of protein aggregated at the base of the wells and failed to migrate into the gel. Optimizing gel shift assay conditions to allow the migration of protein into the gel proved difficult. Instead, β-galactosidase assays were performed as an alternative to assess potential binding sites of the *ptrA* promoter. A decrease in

transcriptional activity was observed when the region between 52 and 198 bp upstream of the translational start site was truncated; positive autoregulatory elements may lie within that region.

4. 5. Future directions

The lack of LTTR structural data continues to limit our understanding of the largest family of bacterial transcriptional regulators. The autoregulatory role of *ptrA* is still not clear, and the identity of the co-inducer molecule and the PtrA-regulated target genes are not known. Solving the structure of the effector binding domain will help identify the co-inducer molecule. The truncated version of the protein, however, is not a functional protein. The more desirable goal would be to solve the structure of full-length PtrA. The solubility issues associated with PtrA will need to be resolved. In doing so, DNA-binding experiments such as gel shifts and footprinting may be successfully performed to identify PtrA binding sites.

A full-length LTTR protein bound to a natural co-inducer or DNA has yet to be solved. Long-term goals involve the co-crystallization of the full-length PtrA structure with DNA and co-inducer molecules. Defining the co-inducer molecule and genes regulated by *ptrA* will improve our understanding of how the transcriptional regulator fits within the overall regulatory networks of PA23. Continuing research on PtrA will improve our knowledge of LTTRs, and help optimize *P. chlororaphis* PA23 as a biological control agent.

REFERENCES

Abd-Elgawad, M.M., El-Mougy, N.S., El-Gamal, N.G., Abdel-Kader, M.M., Mohamed, M.M. (2010) Protective treatments against soilborne pathogens in citrus orchards. *J Plant Prot Res.* **50**:477-484.

Adams, P.B. and Ayers, W.A. (1979) Ecology of Sclerotinia species. *Phytopathology*. **69:**896–898.

Akakura, R. and Winans, S.C. (2002a) Mutations in the *occQ* operator that decrease OccR-induced DNA bending do not cause constitutive promoter activity. *J Biol Chem.* **277**:15773–15780.

Akakura, R. and Winans, S.C. (2002b) Constitutive mutations of the OccR regulatory protein affect DNA bending in response to metabolites released from plant tumors. *J Biol Chem*. **277**:5866–5874.

Alibolandi, M., and Mirzahoseini, H. (2011) Chemical Assistance in Refolding of Bacterial Inclusion Bodies. *Biochem Res Int.* **2011**:631607.

Arnold, K., Bordoli, L., Kopp, J., Schwede, T. (2006) The SWISS-MODEL Workspace: A web-based environment for protein structure homology modelling. *Bioinformatics.* **22:**195-201.

Aust, S.D., Morehouse, L.A., Thomas, C.E. (1985) Role of metals in oxygen radical reactions. *Journal of Free Radicals in Biology and Medicine.* **1**:3-25.

Axler-DiPerte, G.L., Hinchliffe, S.J., Wren, B.W., Darwin, A.J. (2009) YtxR acts as an overriding transcriptional off switch for the *Yersinia enterocolitica* Ysc-Yop type 3 secretion system. *J Bacteriol.* **191**:514–524.

Bergfors, T. (2003) Seeds to crystals. *J Struct Biol*. **142**:66-76.

Burgess, R.R. (1991) Use of polyethyleneimine in purification of DNA-binding proteins. *Methods Enzymol.* **208**:3–10.

Bertani, I., and Venturi, V. (2004) Regulation of the N-Acyl Homoserine Lactone-Dependent Quorum-Sensing System in Rhizosphere *Pseudomonas putida* WCS358 and Cross-Talk with the Stationary-Phase RpoS Sigma Factor and the Global Regulator GacA. *Appl Environ Microbiol*. **70**:5493–5502.

Boland, G.J., and Hall, R. (1994) Index of plant hosts of *Sclerotinia sclerotiorum*. *Can J Plant Pathol.* **16**:93–108.

Boller, T. (1995) Chemoperception of microbial signals in plant cells. *Annu. Rev. Plant Physiol Plant Mol Biol.* **46**:189-214.

Bourot, S., Sire, O., Trautwetter, A. (2000) Glycine betaine-assisted protein folding in a *lysA* mutant of *Escherichia coli*. *J Biol Chem.* **275**:1050–1056.

Bradley, C.A., Lamey, H.A., Endres, G.J., Henson, R.A., McKay, K., Halvorson, M., LeGare, D.G., Porter, P.M. (2006) Efficacy of fungicides for control of Sclerotinia stem rot of canola. *Plant Disease*. **90**:1129-1134.

Canola Council of Canada. (1999) Canola – The Official Definition. Available from http://www.canolacouncil.org/ind_definition.aspx: [cited May 2012]

Canola Council of Canada. (2005) Canola Quick Facts. Available from http://www.canolacouncil.org/facts_export.aspx: [updated Nov 2005; cited May 2012]

Cao, H., Krishnan, G., Goumnerov, B., Tsongalis, J., Tompkins, R., Rahme, L.G. (2001) A quorum sensing-associated virulence gene of *Pseudomonas aeruginosa* encodes a LysR-like transciprtional regulator with a unique self-regulatory mechanism. *Microbiology.* **98**:14613-14618.

Cessna, S.G., Sears, V.E., Dickman, M.B., Low, P.S. (2000) Oxalic acid, a pathogenicity factor for *Sclerotinia sclerotiorum*, suppresses the oxidative burst of the host plant. *Plant Cell*. **12**:2191–2200.

Chancey, S.T., Wood, D.W., Pierson, L.S. (1999) Two component transcriptional regulation of *N*-acyl-homoserine lactone production in *Pseudomonas aureofaciens*. *Appl Environ Microbiol*. **65**:2294–2299.

Chayen, N.E., and Saridakis, E. (2008) Protein crystallization: from purified protein to diffraction-quality crystal. *Nature Methods.* **5:**147-153.

Chen, C., Belanger, R.R., Benhameu, N., Paulitz, T.C. (2000) Defense enzymes induced in cucumber roots by treatment with plant growth promoting rhizobacteria. *Physiol. Mol Plant Pathol.* **56**:13–23.

Chin-A-Woeng, T.F., Bloemberg, G.V., Mulders, I.H., Dekkers, L.C., Lugtenberg, B.J. (2000) Root colonization by phenazine-1-carboxamide-producing bacterium *Pseudomonas chlororaphis* PCL1391 is essential for biocontrol of tomato foot and root rot. *Mol Plant Microbe Intearct.* **13**:1340-1345.

Chin-A-Woeng, T.F.C., van den Broek, D., de Voer, G., van der Drift, K.M.G.M., Tuinman, S., Thomas-Oates, J.E., Lugtenberg, B.J.J., Bloemberg, G.V. (2001) Phenazine-1-carboxamide production in the biocontrol strain *Pseudomonas chlororaphis* PCL1391 is regulated by multiple factors secreted into the growth medium. *Mol Plant Microbe Interact.* **14**:969-979.

Clark, E.D. (1998) Refolding of recombinant proteins. *Curr Opin Biotechnol*. **9**:157–163.

Collins, B., Stevens, R.C., Page, R. (2005) Crystallization Optimum Solubility Screening: using crystallization results to identify the optimal buffer for protein crystal formation. *Acta Crystallogr Sect F Struct Biol Cryst Commun.* **1**:1035–1038.

Cook, R. J., Chairman. (1987) Research Briefing Panel on Biological Control in Managed Ecosystems. Committee on Science, Engineering, and Public Policy, National Academy of Sciences, National Academy of Engineering, and Institute of Medicine. National Academy Press, Washington, DC. pp. 1-12.

Cook, R.J., and Baker, K.F. (1983) The Nature and Practice of Biological Control of Plant Pathogens. St. Paul, MN: APS Press.

de Vos, G.F., Walker, G.C., Signer, E.R. (1986) Genetic manipulations in Rhizobium meliloti utilizing two new transposon Tn5 derivatives. *Mol Gen Genet.* **204**:485-491.

Dechavanne, V., Barrillat, N., Borlat, F., Hermant, A., Magnenat, L., Paquet, M., Antonsson, B., Chevalet, L. (2011) A high-throughput protein refolding screen in 96-well format combined with design of experiments to optimize the refolding conditions. *Protein Expression and Purification*. **75**:192-203.

Duffy, B.K., and Défago, G. (1999) Environmental factors modulating antibiotic and siderophore biosynthesis by *Pseudomonas fluorescens* biocontrol strains. *Appl Environ Microb*. **65**:2429–2438.

Durrant, W.E., and Dong, X. (2004) Systemic acquired resistance. *Annu Rev Phytopathol.* **42**:185-209.

Ezezika, O.C., Collier-Hyams, L.S., Dale, H.A., Burk, A.C., Neidle, E.L. (2006). CatM regulation of the *benABCDE* operon: functional divergence of two LysR-type paralogs in *Acinetobacter baylyi* ADP1. *Appl Environ Microbiol.* **72**:1749–1758.

Ezezika, O.C., Haddad, S., Clark, T.J., Neidle, E.L., Momany, C. (2007a) Distinct effector binding sites enable synergistic transcriptional activation by BenM, a LysR-type regulator. *J Mol Biol.* **367**:616-629.

Ezezika, O.C., Haddad, S., Neidle, E.L., Momany, C. (2007b) Oligomerization of BenM, a LysR-type transcriptional regulator: structural basis for the aggregation of proteins in this family. *Acta Crystallograph Sect F Struct Biol Cryst Commun* **63**:361-368

Fernando, W. G. D., Ramarathnam, R., Krishnamoorthy, A.S., Savchuk, S.C. (2005) Identification and use of potential bacterial organic antifungal volatiles in biocontrol. *Soil Biology and Biochemistry.* **37**:955–964.

Fernando, W.G.D., Nakkeeran, S.K., Zhang, Y. (2004) Ecofriendly methods in combating *Sclerotinia sclerotiorum* (Lib.) de Bary. *Recent Research Developments in Environmental Biology.* **1**:329–347.

Fernando, W.G.D., Nakkeeran, S.K., Zhang, Y., Savchuck, S.C. (2007) Biological control of *Sclerotinia sclerotiorum* (Lib.) de Bary by *Pseudomonas* and *Bacillus* species on canola petals. *Crop Protection.* **26**:100–107.

Fgaier, H. and Eberl, H.J. (2011) Antagonistic control of microbial pathogens under iron limitations by siderophore producing bacteria in a chemostat setup. *J Theor Biol.* **273**:103-114.

Finan, T.M., Kunkel, B., de Vos, G.F., Signer, E.R. (1986) Second symbiotic megaplasmid in Rhizobium meliloti carrying exopolysaccharide and thiamine synthesis genes. *J Bacteriol.* **167**:66–72.

Fisher R.F., and Long, S.R. (1993) Interactions of NodD at the nod box: NodD binds to two distinct sites on the same face of the helix and induces a bend in the DNA. *J Mol Biol.* **233**:336–348.

Fuller, P., Coyne, D., Steadman, J. (1984) Inheritance of resistance to white mold disease in a diallel cross of dry beans. *Crop Sci.* **24**:929–933.

Ganeshan, G. and Kumar, A.M. (2005) *Pseudomonas fluorescens*, a potential bacterial antagonist to control plant diseases. *J Plant Interact*. **1**:123-134.

Gao, X., Tang, K.J., Wang, L.H., Zhu, B.P. (2009) Research progress of *Sclerotinia sclerotiorum* IPM in China. *Chin Plant Prot.* **29**:15-18.

Gasteiger, E. GA, Hoogland, C., Ivanyi, I., Appel, R.D., Bairoch, A. (2003) ExPASy: the proteomics server for in-depth protein knowledge and analysis. *Nucleic Acids Res.* **31**:3784-8.

Gasteiger, E. HC., Gattiker, A., Duvaud, S., Wilkins, M.R., Appel, R.D., Bairoch, A. (2005) Protein Identification and Aanlysis Tools on the ExPASy Server. In: Walker JM, editor. The Proteomics Protocols Handbook. New York: Humana Press. pp. 571-607.

Ge, Y., Yang, S., Fang, Y., Yang, R., Mou, D., Cui, J., Wen, L. (2007) RpoS as an intermediate in RsmA-dependent regulation of secondary antifungal metabolites biosynthesis in *Pseudomonas* sp. M18. *FEMS Microbiology Letters.* **268**: 81–87.

Gerlagh, M., Goosen-van de Geijn, H.M., Fokkemma, N.J., Vereijken, P.F.G. (1999) Long-term biosanitation by application of *Coniothrium minitans* on *Sclerotinia sclerotiorum*-infected crops. *Phytopathology.* **89**:141–147.

Gilmour, G. (2001) Canola growers losing Benlate fungicide. *Manitoba Cooperator.* **58:**1.

Girard, G., van Rij, E.T., Lugtenberg, B.J., and Bloemberg, G.V. (2006) Regulatory roles of *psrA* and *rpoS* in phenazine-1-carboxamide synthesis by *Pseudomonas chlororaphis* PCL1391. *Microbiology*. **152**:43–58.

Godoy, G., Steadman, J.R., Dickman, M.B., Dam, R. (1990) Use of mutants to demonstrate the role of oxalic acid in pathogenicity of *Sclerotinia sclerotiorum* on Phaseolus vulgaris. *Physiol Mol Plant Pathol.* **37:**179–191.

Gómez-Gómez, L. (2004) Plant perception systems for pathogen recognition and defense. *Mol Immunol.* **41**:1055–1062.

Green, A.A., and Hughes, W.L. (1955) Methods in Enzymology. *Methods Enzymol.* **1**:67-90.

Grob, P., and Guiney, D.G. (1996) In vitro binding of the Salmonella dublin virulence plasmid regulatory protein SpvR to the promoter regions of *spvA* and *spvR*. *J Bacteriol.* **178**:1813–1820.

Guy, R.L., Gonias, L.A., and Stein, M.A. (2000) Aggregation of host endosomes by *Salmonella* requires SPI2 translocation of SseFG and involves SpvR and the *fms–aroE* intragenic region. *Mol Microbiol.* **37**:1417–1435.

Haas, D. and Keel, C. (2003) Regulation of antibiotic production in root-colonizing *Pseudomonas* spp. and relevance for biocontrol of plant disease. *Annu Rev Phytopathol.* **41**:117–153.

Haas, D., and Défago, G. (2005) Biological control of soil-borne pathogens by fluorescent pseudomonads. *Nat Rev Microbiol.* **3**:307-319.

Hammond-Kosack, K.E., and Parker, J.E. (2003) Deciphering plant-pathogen communication: fresh perspectives for molecular resistance breeding. *Curr Op Biotech.* **14**:177-193.

Harris, S.J., Shih, Y.L., Bentley, S.D., and Salmond, G.P. (1998) The *hexA* gene of *Erwinia carotovora* encodes a LysR homologue and regulates motility and the expression of multiple virulence determinants. *Mol Microbiol.* **28**:705–717.

Hedke, K., Luth, P., von Tiedemann (1999) A. Contans – first biocontrol agent against *Sclerotinia sclerotiorum* in oilseed rape. In the Proceedings of the 10th International Rapeseed Congress. September 2001. Canberra, Austrailia.

Heeb, S., Blumer, C., Haas, D. (2002) Regulatory RNA as mediator in GacA/RsmA-dependent global control of exoproduct formation in *Pseudomonas fluorescens* CHA0. *Journal Of Bacteriology.* **184**:1046-56.

Heeb, S., and Haas, D. (2001) Regulatory roles of the GacS/GacA two-component system in plant-associated and other Gram-negative bacteria. *Mol Plant Microbe Interact.* **14**:1351–1363.

Henikoff, S., Haughn, G.W., Calvo, J.M., Wallace, J.C. (1988) A large family of bacterial activator proteins. *Proc Natl Acad Sci USA.* **85**:6602–6606.

Heroven, A.K., and Dersch, P. (2006) RovM, a novel LysR-type regulator of the virulence activator gene *rovA*, controls cell invasion, virulence and motility of *Yersinia pseudotuberculosis*. *Mol Microbiol.* **62**:1469–1483.

Howe, P.W.A. (2004) A straight-forward method of optimising protein solubility for NMR. *J Biomol NMR*. **30**:283-286.

Hryniewicz, M.M., Kredich, N.M. (1995) Hydroxyl radical footprints and half-site arrangements of binding sites for the CysB transcriptional activator of *Salmonella typhimurium*. *J Bacteriol.* **177**:2343–2353.

Huang, X., Zhang, X., Xu, Y. (2008) PltR expression modulated by the global regulators GacA, RsmA, LasI and RhlI in *Pseudomonas* sp. M18. *Res Microbiol.* **159**:128-36.

Hunter, S., Jones, P., Mitchell, A., Apweiler, R., Attwood, T.K., Bateman, A., Bernard, T., Binns, D., Bork, P., Burge, S., et al. (2012) InterPro in 2011: New developments in the family and domain prediction database. *Nucleic Acids Res.* **40**:306-312.

Jancarik, J., Pufan, R., Hong, C., Kim, S.-H., Kim, R. (2004). Optimum solubility (OS) screening: an efficient method to optimize buffer conditions for homogeneity and crystallization of proteins. *Acta Crystallographica.* **60**:1670–1673.

Jiang, M.L., Zhao, R., Hu, X.J., Zhang, Y.B., Wang, G.P. (2007) Colonization of antifungal endobacterium BY-2 in oilcrop rape and its control effect on disease caused by *Sclerotinia sclerotiorum*. *Acta Phytopath Sinica.* **37**:192-196.

Keen, N. T., Tamaki, S., Kobayashi, D., Trollinger, D. (1988) Improved broad-host-range plasmids for DNA cloning in gram-negative bacteria. *Gene*. **70**:191–197.

Khan, S.R., Mavrodi, D.V., Jog, G.J., Suga, H., Thomashow, L.S., Farrand, S. K. (2005) Activation of the *phz* operon of *Pseudomonas fluorescens* 2-79 requires the LuxR

homolog PhzR, N-(3-OH-hexanoyl)-l-homoserine lactone produced by the LuxI homolog PhzI, and a cis-acting *phz* box. *J Bacteriol.* **187**:6517–6527.

Kiefer, F., Arnold, K., Künzli, M., Bordoli, L., Schwede, T. (2009) The SWISS-MODEL Repository and associated resources. *Nucleic Acids Research*. **37**:387-392.

Knapp, G.S., and Hu, J.C. (2010) Specificity of the *E. coli* LysR-type transcriptional regulators. *PLoS ONE*. **5**:e15189

Kovacikova, G., and Skorupski, K. (1999) A *Vibrio chloerae* LysR homolog, AphB, cooperates with AphA at the *tcpPH* promoter to activate expression of the ToxR virulence cascade. *J Bacteriol.* **181**:4250-4256

Kozlovski, V.I., Donald, L.J., Montero-Collado, V., Spicer, V., Loboda, A.V., Chernushevich, I.V., et al. (2005) Proceedings of the 53rd ASMS Conference on Mass Spectrometry and Allied Topics. San Antonio, TX, USA.

Laemmli, U.K. (1970) Cleavage of structural proteins during the assembly of the head of bacteriophage T4. *Nature.* **227**:680–685.

Lapouge, K., Schubert, M., Allain, F.H.-T., Haas, D. (2008) Gac/Rsm signal transduction pathway of γ-proteobacteria: from RNA recognition to regulation of social behaviour. *Mol Microbiol.* **67**:241-253.

Law, A.M., Bains, J., Boulanger, M.J. (2009) Purification and crystallization of a putative transcriptional regulator of the benzoate oxidation pathway in *Burkholderia xenovorans* LB400. *Acta Cryst.* **65**:1001-1003.

Laxalt, A.M., Munnik, T. (2002) Phospholipid signalling in plant defense. *Curr Opin Plant Biol*. **5**:332–38.

Layne, E. (1957) Spectrophotometric and turbidimetric methods for measuring proteins. *Methods Enzymol.* **3**:447-454.

Lehnen, D., Blumer, C., Polen, T., Wackwitz, B., Wendisch, V.F., and Unden, G. (2002) LrhA as a new transcriptional key regulator of flagella, motility and chemotaxis genes in *Escherichia coli*. *Mol Microbiol*. **45**:521–532.

Li, H., Li, H., Bai, Y., Wang, J., Nie, M., Bi, B., Xiao, M. (2011) The Use of *Pseudomonas fluorescens* P13 to Control Sclerotinia Stem Rot (*Sclerotinia sclerotiorum*) of Oilseed Rape. *The Journal of Microbiology*. **49:**884-889.

Li, Y., He, Z-G. (2012) The Mycobacterial LysR-Type Regulator OxyS Responds to Oxidative Stress and Negatively Regulates Expression of the Catalase-Peroxidase Gene. *PLoS ONE.* **7**:e30186.

Li, Y.B., Yongli, Z., and Nian, L.B. (1994) Study on the dissemination distance of sunflower stem rot fungus. *Plant Prot*. **20**:12–13.

Lindquist, S., Lindberg, F., Normark, S. (1989) Binding of the *Citrobacter freundii* AmpR regulator to a single DNA site provides both autoregulation and activation of the inducible *ampC* beta-lactamase gene. *J Bacteriol.* **71**:3746-3753.

Liu, Y., Cui, Y., Mukherjee, A., Chatterjee, A.K. (1998) Characterization of a novel RNA regulator of *Erwinia carotovora* subsp. *Carotovora* that controls production of extra-cellular enzymes and secondary metabolites. *Mol Microbiol.* **29**:219-234.

Liu, S., Wang, H., Zhang, J., Fitt, B. D., Xu, Z., Evans, N., Liu, Y., Yang, W., and Guo, X. (2005) In vitro mutation and selection of doubled-haploid *Brassica napus* lines with improved resistance to *Sclerotinia sclerotiorum*. *Plant Cell Rep.* **24**:133-144.

Lopez-Sanchez, A., Rivas-Marin, E., Martinez-Perez, O., Floriano, B., Santero, E. (2009) Coordinated regulation of two divergent promoters through higher-order complex formation by the LysR-type regulator ThnR. *Mol Microbiol*. **73**:1086-1100.

Lorenz, E., Stauffer, G.V. (1995) Characterization of the MetR binding sites for the *glyA* gene of *Escherichia coli. J. Bacteriol.* **177**:4113–4120.

Maachupalli-Reddy, J., Kelly, B.D., de Bernardez Clark, E. (1997) Effect of inclusion body contaminants on the oxidative renaturation of hen egg white lysozyme. *Biotechnol Prog.* **13**:144–150.

Maddocks, S.E., and Oyston, P.C.F. (2008) Structure and function of the LysR-type transcriptional regulator (LTTR) family proteins. *Microbiology*. **154**:3609-3623.

Manitoba Agriculture, Food and Rural Initiatives. (2004) Sclerotinia in Canola. Available from http://www.gov.mb.ca/agriculture/crops/diseases/fac07s00.html: [updated May 2008; cited May 2012]

Manuel, J., Selin, C., Fernando, W.G.D., de Kievit, T. (2012) Stringent response mutants of *Pseudomonas chlororaphis* PA23 exhibit enhanced antifungal activity against *Sclerotinia sclerotiorum* in vitro. Microbiology. **158**:207-16.

Marciano, P., DiLenna, P., Magro, P. (1983) Oxalic acid, cell wall degrading enzymes and pH in pathogenesis and their significance in the virulence of two *Sclerotinia sclerotiorum* isolates on sunflower. *Physiol Plant Pathol.* **22:**339–345.

Marshall, D.G., Sheehan, B.J., and Dorman, C.J. (1999) A role for the leucine-responsive regulatory protein and integration host factor in the regulation of the Salmonella plasmid virulence (spv) locus in *Salmonella typhimurium*. *Mol Microbiol*. **34**:134–145.

Martens, J.W., Seaman, W.L., Atkinson, T.G. (1994) Disease of canola, rapeseed, and mustard. Diseases of field crops in Canada. pp. 116-121.

McDowell, J.M., and Dangl, J.L. (2000) Signal transduction in the plant immune response. *Trends Biochem. Sci.* **25**:79–82.

McLaren, D., Huang, H., Rimmer, S. (1996) Control of apothecia production of *Sclerotinia sclerotiorum* by *Coniothyrium minitans* and *Talaromyces flavus*. *Plant Dis.* **80**:1373–1378.

McQuilken, M.P., Mitchell, S.J., Budge, S.P., Whipps, J.M., Fenlon, J.S., Archer, S.A. (1995) Effect of *Coniothyrium minitans* on sclerotial survival and apothecial production of *Sclerotinia sclerotiorum* in field-grown oilseed rape. *Plant Pathology*. **44**:883:896.

Miller, J.H. (1972) "Experiments in molecular genetics." Cold Spring Harbor Laboratory, Cold Spring Harbor, NY.

Momany, C., and Neidle, E.L. (2012) Defying stereotypes: the elusive search for a universal model of LysR-type regulation. *Mol Microbiol*. **83**:453-456.

Monferrer, D., Tralau, T., Kertesz, M.A., Dix, I., Sola, M., Uson, I. (2010) Structural studies on the full-length LysR-type regulator TsaR from *Comamonas testosteroni* T-2 reveal a novel open conformation of the tetrameric LTTR fold. *Mol Microbiol.* **75**:1199-1214.

Monferrer, D., Tralau, T., Kertesz, M.A., Panjikar, S., Usón, I. (2008) High crystallizability under air-exclusion conditions of the full-length LysR-type transcriptional regulator TsaR from Comamonas testosteroni T-2 and data-set analysis for a MIRAS structure solution approach. *Acta Crystallogr Sect F Struct Biol Cryst Commun.* **64**:764–769.

Morrall, R.A.A., and Dueck, J. (1982) Epidemiology of sclerotinia stem rot of rapeseed in Saskatchewan *Sclerotinia sclerotiorum, Brassica napus, Brassica campestris*. *Can J. Plant Pathol.* **4**:161-168.

Mukherjee, A., Cui, Y., Ma, W., Liu, Y., Chatterjee, A.K. (2000) *hexA* of Erwinia *carotovora* ssp. *carotovora* strain Ecc71 negatively regulates production of RpoS and rsmB RNA, a global regulator of extracellular proteins, plant virulence and the quorum-sensing signal, N-(3-oxohexanoyl)-L-homoserine lactone. *Environ Microbiol.* **2**:203–215.

Muraoka, S., Okumura, R., Ogawa, N., Nonaka, T., Miyashita, K., Senda, T. (2003) Crystal structure of a full-length LysR-type transcriptional regulator, CbnR: unusual combination of two subunit forms and molecular bases for causing and changing DNA bend. *J Mol Biol.* **328**:555-566.

Nakkeeran, S., Kavitha, K., Chandrasekar, G., Renukadevi, P., Fernando, W.G.D. (2006) Induction of plant defence compounds by *Pseudomonas chlororaphis* PA23 and *Bacillus subtilis* BSCBE4 in controlling damping-off of hot pepper caused by *Pythium aphanidermatum*. *Biocontrol Science and Technology.* **16**:403–416.

Nelson, B. (1998) Biology of Sclerotinia. In: Proceedings of the 10th International Sclerotinia workshop, 21 Jan. 1998. North Dakota State University Department of Plant Pathology, Fargo, ND. pp. 1–5.

O'Grady, E.P., Nguyen, D.T., Weisskopf, L., Eberl, L., Sokol, P.A. (2011) The *Burkholderia cenocepacia* LysR-type transcriptional regulator ShvR influences expression of quorum-sensing, protease, type II secretion, and afc genes. *J Bacteriol.* **193**:163–176.

Pareja, E., Pareja-Tobes, P., Manrique, M., Pareja-Tobes, E., Bonal, J., Tobes, R. (2006) ExtraTrain: a database of extragenic regions and transcriptional information in prokaryotic organisms. *BMC Microbiol* **6**:29.

Parsek, M.R., Kivisaar, M., Chakrabarty, A.M. (1995) Differential DNA bending introduced by the *Pseudomonas putida* LysR-type regulator, CatR, at the plasmid-borne *pheBA* and chromosomal *catBC* promoters. *Mol Microbiol.* **15**:819–828.

Parsek, M.R., Shinabarger, D.L., Rothmel, R.K., Chakrabarty, A.M. (1992) Roles of CatR and cis,cis-muconate in activation of the *catBC* operon, which is involved in benzoate degradation in *Pseudomonas putida*. *J Bacteriol.* **174**:7798–7806.

Parsek, M.R., Ye, R.W., Pun, P., Chakrabarty, A.M. (1994) Critical nucleotides in the interaction of a LysR-type regulator with its target promoter region *catBC* promoter activation by CatR. *J Biol Chem.* **269**:11279-11284.

Peitsch, M.C. (1995) Protein modeling by E-mail. *Bio/Technology.* **13**:658-660.

Picossi, S., Belitsky, B.R., Sonenshein, A.L. (2007) Molecular mechanisms of the regulation of *Bacillus subtilis gltAB* expression by GltC. *J Mol Biol.* **365**:1298-1313.

Pineiro, S., Olekhnovich, I., Gussin, G.N. (1997) DNA bending by the TrpI protein of *Pseudomonas aeruginosa. J Bacteriol.* **179**:5407–5413.

Pope, S.J., Varney, P.L., Sweet, J.B. (1989) Susceptibility of cultivars of oilseed rape to *Sclerotinia sclerotiorum* and the effect of infection on yield. *Asp Appl Biol.* **23**:451–456.

Poritsanos, N.J. (2005) Molecular mechanisms involved in secondary metabolite production and biocontrol of *Pseudomonas chlororaphis* PA23. MSc. Thesis, University of Manitoba.

Porrúa, O., García-Jaramillo, M., Santero, E., Govantes, F. (2007) The LysR-type regulator AtzR binding site: DNA sequences involved in activation, repression and cyanuric acid-dependent repositioning. *Mol Microbiol.* **66**:410–427.

Porrúa O, Platero, A.I., Santero, E., del Solar, G., Govantes, F. (2010) Complex interplay between the LysR-type regulator AtzR and its binding site mediates atzDEF activation in response to two distinct signals. *Mol Microbiol*. **76**:331-47.

Purdy, L.H. (1979) *Sclerotinia sclerotiorum*: history, diseases and symptomatology, host range, geographic distribution, and impact. *Phytopathology*. **69**:875-880.

Reimmann, C., Beyeler, M., Latifi, A., Winteler, H., Foglino, M., Lazdunski, A., Haas, D. (1997) The global activator GacA of *Pseudomonas aeruginosa* PAO positively controls the production of the autoinducer *N*-butyryl-homoserine lactone and the formation of the virulence factors pyocyanin, cyanide, and lipase. *Mol Microbiol*. **24**:309–319.

Religa, T.L., Johnson, C.M., Vu, D.M., Brewer, S.H., Dyer, R.B., Fersht, A.R. (2007) The helix–turn–helix motif as an ultrafast independently folding domain: The pathway of folding of Engrailed homeodomain. *Proc. Natl Acad. Sci. USA.* **104**:9272–9277.

Ren, L., Liu, H.P., Han, J.C., Xing, K. (2007) Preliminary studies on antagonistic action of endophytic bacteria yc8 to *Sclerotinia sclerotiorum*. *J Anhui Agric Sci.* **35:**3294-3295.

Romeis, T. (2001) Protein kinases in the plant defence response. *Curr Opin Plant Biol.* **4**:407–414.

Ruangprasert, A., Craven, S.H., Neidle, E.L., Momany, C. (2010) Full-length structures of BenM and two variants reveal different oligomerization schemes for LysR-Type transcriptional regulators. *J Mol Biol.* **404**:568–586.

Sainsbury, S., Lane, L.A., Ren, J., Gilbert, R.J., Saunders, N.J., Robinson, C.V., Stuart, D.I., Owens, R.J. (2009) The structure of CrgA from *Neisseria meningitidis* reveals a new octameric assembly state for LysR transcriptional regulators. *Nucleic Acids Res.* **37**:4545-4558.

Sainsbury, S., Ren, J., Saunders, N.J., Stuart, D.I., Owens, R.J. (2008) Crystallization and preliminary X-ray analysis of CrgA, a LysR-type transcriptional regulator from pathogenic *Neisseria meningitidis* MC58. *Acta Crystallogr Sect. F.* **64**:797–801.

Saharan, B.S., Nehra, V. (2011) Plant growth promoting rhizobacteria: A critical review. *Life Sciences and Medicine Research.* **21**:1-30.

Sambrook, J., Fritsch, E.F., and Maniatis, T. (1989) Molecular Cloning: A Laboratory Manual. Cold Harbour Laboratory. Cold Spring Harbour Press. New York.

Sarniguet, A., Kraus, J., Henkels, M.D., Muehlchen, A.M., Loper, J.E. (1995) The sigma factor s affects antibiotic production and biological control activity of *Pseudomonas fluorescens* Pf-5. *Proc Natl Acad Sci USA.* **92:**12255–12259.

Savchuk, S.C. (2002) Evaluation of biological control control of *Sclerotinia sclerotiorum* on Canola (*Brassica napus*) in the lab, in the greenhouse, and in the field. MSc. thesis, University of Manitoba.

Savchuk, S.C., Fernando, W.G.D. (2004) Effect of timing of application and population dynamics on the degree of biological control of *Sclerotinia sclerotiorum* by bacterial antagonists. *FEMS Microbiol Ecol.* **49**:379–388.

Schell, M.A. (1993) Molecular biology of the LysR family of transcriptional regulators. *Annu Rev Microbiol.* **47**:597-626.

Schell, M.A., and Poser, E.F. (1989) Demonstration, characterization, and mutational analysis of NahR protein binding to *nah* and *sal* promoters. *J Bacteriol.* **171**:837–846.

Schnider, U., Keel, C., Blumer, C., Troxler, J., Defago, G., Haas, D. (1995) Amplification of the housekeeping sigma factor in *Pseudomonas fluorescens* CHA0 enhances antibiotic production and improves biocontrol abilities. *J Bacteriol.* **177**:5387-5392.

Schuster, M., Urbanowski, M.L., Greenberg, E.P. (2004) Promoter specificity in *Pseudomonas aeruginosa* quorum sensing revealed by DNA binding of purified LasR. *Proc Natl Acad Sci USA*. **101**:15833–15839.

Selin, C., Habibian, R., Poritsanos, N., Athukorala, S.N.P., Fernando, W.G.D., de Kievit, T.R. (2009) Phenazines are not essential for Pseudomonas chlororaphis PA23 biocontrol of *Sclerotinia sclerotiorum*, but do play a role in biofilm formation. *FEMS Microbiol Ecol.* **71**:73–83.

Shi, J.L., Li, Y., Qian, L.H., Du, G.C., Chen, J. (2004) *Coniothyrium minitas* CCTCC M203020: its characteristics and potential in biological control of *Sclerotinia sclerotiorum* in oilseed rape. *Chin J Appl Environ Biol.* **10**:798-802.

Silby, M.W., Giddens, S.R., Mahanty, H.K. (2005) Mutation of a LysR-type regulator of antifungal activity results in a growth advantage in stationary phase phenotype in *Pseudomonas aureofaciens* PA147-2. *Appl Environ Microbiol.* **71**:569–573.

Singh, S.M., and Panda, A.K. (2005) Solubilization and refolding of bacterial inclusion body proteins. *Journal of Bioscience and Bioengineering*. **99**:303-310.

Slininger, P.J., and Shea-Wilbur, M.A. (1995) Liquid-culture pH, temperature, and carbon (not nitrogen) source regulate phenazine productivity of the take-all biocontrol agent *Pseudomonas fluorescens* 2–79. *Appl Microbiol Biotechnol.* **43**:794-800.

Smirnova, I.A., Dian, C., Leonard, G.A., McSweeney, S., Birse, D., Brzezinski, P. (2004) Development of a bacterial biosensor for nitrotoluenes: the crystal structure of the transcriptional regulator DntR. *J Mol Biol.* **340**:405-418.

Suh, S.J., Silo-Suh, L., Woods, D.E., Hassett, D.J., West, S.E.H., Ohman, D.E. (1999) Effect of rpoS Mutation on the Stress Response and Expression of Virulence Factors in *Pseudomonas aeruginosa. J Bacteriol.* **181**:3890-3897.

Sun, J., and Klein, A. (2004) A lysR-type regulator is involved in the negative regulation of genes encoding selenium-free hydrogenases in the archaeon Methanococcus voltae. *Mol Microbiol*. **52**:563–571.

Taylor, J.L., de Silva, R.S., Kovacikova, G., Lin, Wei., Taylor, R.K., Skorupski, K., Kull, F.J. (2012) The crystal structure of AphB, a virulence gene activator from *Vibrio cholerae*, reveals residues that influence its response to oxygen and pH. *Mol Microbiol*. **83**:457-470.

Thomashow, L.S., and Weller, D.M. (1988) Role of a phenazine antibiotic from *Pseudomonas fluorescens* in biological control of *Gaeumannomyces graminis* var. tritici. *J Bacteriol.* **170**:3499-3508.

Toledano, M.B., Kullik, I., Trinh, F., Baird, P.T., Schneider, T.D., Storz, G. (1994) Redox-dependent shift of OxyR-DNA contacts along an extended DNA-binding site: a mechanism for differential promoter selection. *Cell.* **78**:897-909.

Tropel, D., and van der Meer, J.R. (2004) Bacterial transcriptional regulators for degradation pathways of aromatic compounds. *Microbiol Mol Biol Rev.* **68**:474–500.

Tsumoto, K., Ejima, D., Kumagai, I., Arakawa, T. (2003) Practical considerations in refolding proteins from inclusion bodies. *Protein Expr Purif*. **28**:1–8.

Tyrrell, R., Verschueren, K.H., Dodson, E.J., Murshudov, G.N., Addy, C., Wilkinson, A.J. (1997) The structure of the cofactor-binding fragment of the LysR family member, CysB: a familiar fold with a surprising subunit arrangement. *Structure*. **5**:1017–1032.

USDA FAS. United States Department of Agriculture, Foreign Agriculture Service. (2012) Oilseeds: World Markets and Trade. Available from www.Fas.usda.gov/oilseeds/current: [updated May 2012; cited May 2012]

van den Bergh, E.R., Dijkhuizen, L., Meijer, W.G. (1993) CbbR, a LysR-type transcriptional activator, is required for expression of the autotrophic CO2 fixation enzymes of *Xanthobacter flavus. J Bacteriol.* **175**:6097-6104.

van Keulen, G., Girbal, L., van den Bergh, E.R., Dijkhuizen, L., Meijer, W.G. (1998) The LysR-type transcriptional regulator CbbR controlling autotrophic CO2 fixation by *Xanthobacter flavus* is an NADPH sensor. *J Bacteriol.* **180:**1411–1417.

van Loon, L.C., Baker, P.A.H.M., Pieterse, M.J. (1998) Systemic resistance induced by rhizosphere bacteria. *Annu Rev Phytopathol.* **36**:453–483.

van Rij, E.T., Wesselink, M., Chin-A-Woeng, T.F.C., Bloemberg, G.V., Lugtenberg, B.J.J. (2004) Influence of environmental conditions on the production of phenazine-1-carboxamide by *Pseudomonas chlororaphis* PCL1391. *Mol Plant Microbe Interact*. **17**:557–566.

Vedadi, M., Niesen, F.H., Allali-Hassani, A., Fedorov, O.Y., et al. (2006) Chemical screening methods to identify ligands that promote protein stability, protein crystallization, and structure determination. *Proc Natl Acad Sci USA*. **103**:15835–15840.

Viswanathan, P., Ueki, T., Inouye, S., and Kroos, L. (2007). Combinatorial regulation of genes essential for *Myxococcus xanthus* development involves a response regulator and a LysR-type regulator. *Proc Natl Acad Sci USA.* **104:**7969–7974.

Voisard, C., Keel, C., Haas, D., Défago, G. (1989) Cyanide production by *Pseudomonas fluorescens* helps suppress black root rot of tobacco under gnotobiotic conditions. *EMBO J.* **8**:351-358.

Vrije, T.D., Antoine, N., Buitelaar, R.M., Brucker, S., Dissevelt, M., Durand, A., Gerlagh, M., Jones, E.E., Luth, P., Oostra, J. (2001) The fungal biocontrol agent *Coniothyrium minitans*: production by solid-state fermentation, application and marketing. *Appl Microbiol Biotechnol*. **56**:58-68.

Waage, J., and Greathead, D.J. (1988) Biological control: challenges and opportunities. In R. K. S. Wood and M. J. Way (eds.). Biological Control of Pests, Pathogens, a Weeds: Developments and Prospects. The Royal Soc., London. Pp. 1-18.

Wang, L., and Winans, S.C. (1995) The sixty nucleotide OccR operator contains a subsite essential and sufficient for OccR binding and a second subsite required for ligand-responsive DNA bending. *J Mol Biol.* **253**:691-702.

Warburg, O. and Christian, W. (1941) Isolierung und kristallisation des garungsfrements enolase. *Biochemische Zeitschrift.* **310**:384-421.

Weller, D.M. (1988) Biological control of soilborne plant pathogens in the rhizosphere with bacteria. *Ann Rev Phytopathol.* **26**:379-407.

White, K.D. (1970) Roman Farming. *Cornell University Press*. Ithaca, New York, USA.

Whiteley, M., Lee, K.M., Greenberg, E.P. (1999) Identification of genes controlled by quorum sensing in *Pseudomonas aeruginosa*. *PNAS*. **96**:13904-13909.

Williams B., Kabbage M., Kim H-J., Britt R., Dickman M.B. (2011) Tipping the Balance: *Sclerotinia sclerotiorum* Secreted Oxalic Acid Suppresses Host Defenses by Manipulating the Host Redox Environment. *PLoS Pathog.* **7**:e1002107.

Williams, J.R., and Stelfox, D. (1980) Influence of farming practices in Alberta on germination and apothecium production of sclerotia of *Sclerotinia sclerotiorum* causal organism of sclerotinia stem rot and head blight of rapeseed. *Can J Plant Pathol.* **2**:169-172.

Wilson, R.L., Urbanowski, M.L., and Stauffer, G.V. (1995) DNA binding sites of the LysR-type regulator GcvA in the *gcv* and *gcvA* control regions of *Escherichia coli*. *J Bacteriol*. **177**:4940–4946.

Wood, D.W., Pierson, L.S. III. (1996) The phzI gene of *Pseudomonas aureofaciens* 30-84 is responsible for the production of a diffusible signal required for phenazine antibiotic production. *Gene*. **168**:49–53.

Yan, A., Wang, X., Zhang, X., Xu, Y. (2007) LysR family factor PltR positively regulates pyoluteorin production in a pathway-specific manner in *Pseudomonas* sp. M18. *Sci China Ser C Life Sci.* **37**:325-332.

Yu, G.Y., Sinclair, B., Hartman, G.L., Bertagnolli, B.L. (2002) Production of iturin A by *Bacillus amyloliquefaciens* suppressing *Rhizoctonia solani*. *Soil Biol Biochem.* **34**:955-963.

Zhang, W.Q., Nie, M., and Xiao, M. (2007) Advances in biocontrol mechanism of *Psueudomonas fluorescens*. *J Biol*. **3**:9-11.

Zhang, Y. (2004) Biocontrol of Sclerotinia stem rot of canola by bacterial antagonists and study of biocontrol mechanisms involved. MSc. thesis, University of Manitoba.

Zhang, Y., Fernando, W.G.D., de Kievit, T.R., Berry, C., Daayf, F., Paulitz, T.C. (2006) Detection of antibiotic-related genes from bacterial biocontrol agents with polymerase chain reaction. *Can J Microbiol.* **52**:476-81.

Zhang, Z., and Pierson, L.S. (2001) A second quorum-sensing system regulates cell surface properties but not phenazine antibiotic production in *Pseudomonas aureofaciens*. *Appl Environ Microbiol*. **67**:4305-4315.

Zhao, J. and Meng, J. (2003) Genetic analysis of loci associated with partial resistance to *Sclerotinia sclerotiorum* in rapeseed (*Brassica napus* L.). *Theor Appl Genet.* **106**:759–764.

Zhao, J., Peltier, A.J., Meng, J., Osborn, T. Grau, C.R. (2004) Evaluation of Sclerotinia stem rot resistance in oilseed *Brassica napus* using a petiole inoculation technique under greenhouse conditions. *Plant Dis.* **88**:1033–1039.

Zhao, J., Wang, J., An, L., Doerge, R., Chen, Z., Grau, C., Meng, J., Osborn, T.C. (2007) Analysis of gene expression profiles in response to *Sclerotinia sclerotiorum* in *Brassica napus*. *Planta.* **227**:13–24.

Zhou, X., Lou, Z., Fu, S., Yang, A., Shen, H., Li, Z., Feng, Y., Bartlam, M., Wang, H., Rao, Z. (2010) Crystal structure of ArgP from *Mycobacterium tuberculosis* confirms two distinct conformations of full-length LysR transcriptional regulators and reveals its function in DNA binding and transcriptional regulation. *J Mol Biol.* **396**:1012-1024.